Elevated temperature material properties of stainless steel reinforcing bar

L. Gardner[a], Y. Bu[a], P. Francis[b], N. R. Baddoo[b], K.A. Cashell[c] and F. McCann[d],

[a] Imperial College London

[b] The Steel Construction Institute

[c] Brunel University London

[d] London South Bank University

Abstract

Corrosion of carbon steel reinforcing bar can lead to deterioration of concrete structures, especially in regions where road salt is heavily used or in areas close to sea water. Although stainless steel reinforcing bar costs more than carbon steel, its selective use for high risk elements is cost-effective when the whole life costs of the structure are taken into account. Considerations for specifying stainless steel reinforcing bars and a review of applications are presented herein. Attention is then given to the elevated temperature properties of stainless steel reinforcing bars, which are needed for structural fire design, but have been unexplored to date. A programme of isothermal and anisothermal tensile tests on four types of stainless steel reinforcing bar is described: 1.4307 (304L), 1.4311 (304LN), 1.4162 (LDX 2101®) and 1.4362 (2304). Bars of diameter 12 mm and 16 mm were studied, plain round and ribbed. Reduction factors were calculated for the key strength, stiffness and ductility properties and compared to equivalent factors for stainless steel plate and strip, as well as those for carbon steel reinforcement. The test results demonstrate that the reduction factors for 0.2% proof strength, strength at 2% strain and ultimate strength derived for stainless steel plate and strip can also be applied to stainless steel reinforcing bar. Revised reduction factors for ultimate strain and fracture strain at elevated temperatures have been proposed. The ability of two-stage Ramberg-Osgood expressions to capture accurately the stress-strain response of stainless steel reinforcement at both room temperature and elevated temperatures is also demonstrated.

Elevated temperature material properties of stainless steel reinforcing bar

L. Gardner[a], Y. Bu[a], P. Francis[b], N. R. Baddoo[b], K.A. Cashell[c] and F. McCann[d],

[a] Imperial College London

[b] The Steel Construction Institute

[c] Brunel University London

[d] London South Bank University

Highlights

- Review of use of stainless steel reinforcing bars
- Isothermal and anisothermal testing of stainless steel reinforcing bars
- Proposal of reduction factors for key elevated temperature material properties for stainless steel rebar
- Proposal of material models for representing the room and elevated temperature stress-strain response of stainless steel rebar

Elevated temperature material properties of stainless steel reinforcing bar

L. Gardner[a], Y. Bu[a], P. Francis[b], N. R. Baddoo[b], K.A. Cashell[c] and F. McCann[d],

[a] Imperial College London

[b] The Steel Construction Institute

[c] Brunel University London

[d] London South Bank University

Abstract

Corrosion of carbon steel reinforcing bar can lead to deterioration of concrete structures, especially in regions where road salt is heavily used or in areas close to sea water. Although stainless steel reinforcing bar costs more than carbon steel, its selective use for high risk elements is cost-effective when the whole life costs of the structure are taken into account. Considerations for specifying stainless steel reinforcing bars and a review of applications are presented herein. Attention is then given to the elevated temperature properties of stainless steel reinforcing bars, which are needed for structural fire design, but have been unexplored to date. A programme of isothermal and anisothermal tensile tests on four types of stainless steel reinforcing bar is described: 1.4307 (304L), 1.4311 (304LN), 1.4162 (LDX 2101®) and 1.4362 (2304). Bars of diameter 12 mm and 16 mm were studied, plain round and ribbed. Reduction factors were calculated for the key strength, stiffness and ductility properties and compared to equivalent factors for stainless steel plate and strip, as well as those for carbon steel reinforcement. The test results demonstrate that the reduction factors for 0.2% proof strength, strength at 2% strain and ultimate strength derived for stainless steel plate and strip can also be applied to stainless steel reinforcing bar. Revised reduction factors for ultimate strain and fracture strain at elevated temperatures have been proposed. The ability of two-stage Ramberg-Osgood expressions to capture accurately the stress-strain response of stainless steel reinforcement at both room temperature and elevated temperatures is also demonstrated.

Keywords

Anisothermal, Constitutive law, Elevated temperature, Fire design, Reinforced concrete, Rebar, Reinforcing bar, Isothermal, Material modelling, Stainless steel, Stress strain, Structures.

1. Introduction

The traditional approach to improving the durability of reinforced concrete structures is to modify the concrete specification, in terms of composition and/or cover requirements. Whilst this approach can improve

the performance, it is not an inherently durable solution to the problem of chloride-induced corrosion and there is a risk that significant maintenance may be required within the design life of the structure. Maintenance is disruptive and costly, especially when it results in transportation disruptions and/or the loss of production due to facility shut-down. The use of stainless steel reinforcing bar can be a cost-effective option for structures in potentially corrosive environments which are expensive to maintain and repair because stainless steel is highly resistant to corrosion from chloride ions and does not rely on the high alkalinity of concrete for protection. As well as reduced maintenance costs, the use of stainless steel reinforcement will give the structure a longer design life (> 100 years) compared with carbon steel and enable a reduction in concrete cover and weight of deck and substructure.

Stainless steels derive their inherent corrosion resistance from the presence of certain alloying elements, primarily chromium and nickel, which result in differences in microstructure compared to carbon steel. The physical and mechanical properties of stainless steels at room temperature, and at elevated temperatures, also differ from carbon steel. Stainless steels generally retain more of their room temperature strength than carbon steel above temperatures of about 550°C, and more of their stiffness than carbon steel across the whole temperature range [1, 2]. Although there have been a number of investigations into the performance of stainless steel flat material at elevated temperatures, data on the performance of stainless steel reinforcing bar at elevated temperatures are scarce and no information is given in EN 1992-1-2, the Eurocode dealing with the performance of concrete structures at elevated temperatures [3]. This is an important gap in technical knowledge, especially since the protection of key infrastructure elements is becoming increasingly important. As described by Garlock et al. [4], the majority of fires that occur on bridges are hydrocarbon fires, often as a result of spillage from crashed oil tankers. These hydrocarbon fires are characterised by high heating rates, which means failure can occur only a short time after ignition. A notable bridge fire occurred in Birmingham, Alabama in 2002 when a petroleum truck collided with a bridge support at the junction of Interstates 65, 20, and 59. The tanker's cargo ignited, causing a severe fire which damaged the bridge to such an extent that it had to be completely replaced; the consequent traffic disruption was enormously costly [5]. Giuliani et al. [6] studied the vulnerability of bridges to fire and concluded that in the majority of bridge fires, the bridge structure was significantly damaged and high repair costs were sustained. Even where limited structural damage had occurred, high costs due to the temporary closure of the bridge and traffic disruption had to be sustained.

This paper describes the outcomes of a test programme aimed at investigating the elevated temperature material characteristics for stainless steel reinforcement. Two test methods (anisothermal and isothermal) were used to assess the mechanical behaviour at elevated temperatures of plain and ribbed bars of diameter 12 mm and 16 mm in four grades of stainless steel.

2. Applications of stainless steel reinforcing bar

Stainless reinforcing bar was first developed in the 1930's [7] and the earliest known structure with stainless steel reinforcement was the 2100 m long Progreso Pier in the Gulf of Mexico, which was built in 1940 and is

still fit-for-purpose (background, Figure 1). Stainless steel was selected due to the warm and humid marine environment and the use of local limestone aggregate in the concrete with a relatively high porosity. In 1969, a neighbouring pier was built with carbon steel reinforcement which has now suffered very severe corrosion (foreground, Figure 1).

No further applications were found until 1970, when the issue of chloride ingress began to be recognised as a significant problem for reinforced concrete structures in corrosive environments. Since then, stainless steel reinforcing bar has been used around the world in a range of large and small structures including bridges, tunnels, buildings, harbour installations, temples and monuments, both for new structures as well as for repairing corrosion-damaged structures [8]. The non-magnetic property of austenitic stainless steel has also led to the use of stainless steel reinforcing bar in buildings such as hospitals, banks, airports and meteorological stations which house equipment sensitive to magnetic fields.

A more recent example of stainless steel reinforcement being used in a large infrastructure project is in Edmonton, Canada. The very low winter temperatures and high annual snowfall in this area leads to the application of large amounts of salt, both sodium and the more corrosive calcium chloride, to keep the roads as free from ice as possible. Following a successful trial in 2011, around 6000 tonnes of grade 1.4362 duplex stainless steel reinforcing bar were specified for the construction of a new interchange (bridge substructure, retaining walls, overpass etc) on the ring road around the city [8].

Stainless steels are inevitably more expensive than carbon steel due to the alloying elements they contain. In order to realise a whole life cost benefit, it is generally necessary to concentrate stainless steel reinforcing bar in areas of the structure most at risk. Gedge [9] presents a classification system for structural elements that are likely to benefit from specification of stainless reinforcing bar. For the majority of highway bridges, use of stainless steel reinforcing bar for parapet edge beams, bearing shelves on jointed bridges, abutments and intermediate supports adjacent to the carriageway is considered the most cost-effective solution. The United Kingdom's Highway Agency has specifically recognised selective use of stainless steel as a viable option for reduced whole cost of a structure in its *Design Manual for Roads and Bridges* [10]. Predictive models for specifying the level of corrosion resistance required for reinforcing bar in a range of service environments have also been developed [11].

Research by the Virginia Transportation Research Council found that the whole life cost of a bridge that utilises corrosion resistant metallic reinforcing bars (CRR) is substantially less than standard designs with either conventional or epoxy-coated reinforcing bar. As a result, all projects in the State of Virginia with a design life of 75 years or longer are required to use CRR steels and not epoxy coated or galvanised bars [12].

Reinforcing bar is also available in high strength, high chromium microcomposite steels with improved resistance to corrosion, known as MMFX steels [13]. They contain about 9% chromium, so cannot be classified as stainless steel and do not demonstrate the level of corrosion resistance of the standard stainless steels used in the reinforcing bar which are studied in this paper. Another solution for extending the life of reinforced concrete structures exposed to corrosive environments are glass fibre reinforced polymers reinforcing bar. However glass fibre performs poorly at elevated temperatures, and melts at around 800°C.

Numerical modelling has shown that the fire resistance of a beam with carbon steel reinforcing bar is at least double that of an equivalent beam with glass fibre reinforcement [14].

3. Specification of stainless steel reinforcing bar

The sizes of stainless steel reinforcing bars generally range in diameter from 8 mm to 25 mm, and are produced in coils and straight bars cut up to 12 m in length. The two most widely used specifications for stainless steel reinforcement are the British Standard BS 6744 [15] and the American Standard ASTM A955 [16]. These standards both adopt the bar profiles and strength classes given in the British and American carbon steel reinforcing bar standards respectively (EN 10080 [17] and ASTM A615/A615M [18]). The stainless steel material designations in BS 6744 are in accordance with EN 10088-1 [19] and the designations in ASTM A955 are in accordance with ASTM A276 [20].

The test programme described in this paper involved reinforcing bar made from four different grades of stainless steel, which are currently widely used for reinforcing bar, as well as for structural members such as hollow sections, channels, angles, I sections, etc [21-22]. The distinctive characteristics of these steels are given below.

Grade 1.4307 (304L)
This is a low-carbon, standard chromium-nickel austenitic stainless steel. These standard austenitic steels are the most widely used group of stainless steels in construction. Due to its fully austenitic structure, it is suitable for applications with low magnetic permeability requirements.

Grade 1.4311 (304LN)
This is a low-carbon, higher nickel and nitrogen alloyed austenitic stainless steel with improved strength and low-temperature toughness, compared with grade 1.4307. It is also suitable for low magnetic permeability requirements.

Grade 1.4162 (LDX 2101®)
This is a low-nickel, general-purpose duplex stainless steel, known as a ‘lean’ duplex [23, 24]. Duplex stainless steels have approximately twice the strength of austenitic stainless steels. The corrosion resistance of grade 1.4162 is generally as good as the standard chromium-nickel austenitic steels and the reduced nickel content means it also costs about the same also.

Grade 1.4362 (2304)
This is a duplex stainless steel with superior corrosion resistance compared with grade 1.4162, mainly due to the higher content of nickel.

Equivalent designations for these steels are given in Table 1. Note that BS 6744 only lists one standard chromium-nickel austenitic stainless steel, grade 1.4301, with a note permitting the nitrogen content to be increased to a maximum of 0.22%. However, the composition of both grade 1.4307 and grade 1.4311 fall within the compositional limits of grade 1.4301. Guidance on the choice of stainless steel for a given

application is provided in Annex B of BS 6744 [15]; the specific information relating to the grades in the test programme reported herein is reproduced in Table 2.

BS 6744 covers three strength grades: 200, 500 and 650, which correspond to minimum 0.2% proof strengths of 200 MPa, 500 MPa and 650 MPa, respectively. Bars in accordance with the strength grade 500 are most commonly used. ASTM A955 covers two strength classes, grade 60 (yield strength of 420 MPa) and grade 75 (yield strength of 520 MPa).

The strength of austenitic stainless steel bars in the annealed (softened) condition is 175 MPa for grade 1.4307 and 270 MPa for grade 1.4311. The strength of these steels can be increased so that they meet the requirements of either the 200 or 500 strength class in BS 6744 through the addition of cold-work. The strength of duplex stainless steel bars in the annealed condition is 450 MPa for grade 1.4162 and 400 MPa for grade 1.4362. As with the austenitics, the strength of these bars can be increased to either class 500 or class 650 through the addition of cold-work. In the US, in accordance with the terminology used in ASTM A955 [16], austenitic reinforcement is available in grade 60 whereas duplex reinforcing bars are available in grades 60 and 75.

4. Thermal properties of stainless steel

The thermal properties of stainless steels differ from those of carbon steels because of the effect of the differences in microstructure and alloying content. The thermal conductivity of stainless steel and carbon steel [3] are presented in Figure 2; it is noteworthy that the thermal conductivity is the same for austenitic and duplex stainless steels. The low thermal conductivity of stainless steel compared to carbon steel (and copper and aluminium also) has led to the use of stainless steel in thermal breaks and other applications requiring thermal insulation.

The specific heat capacity of stainless steel is compared to carbon steel [3] in Figure 3. The specific heat of the two materials is similar (around 550 to 600 J/kg K), with the exception that carbon steel undergoes a phase change at around 750°C where the microstructure changes from pearlite (a two-phase mixture of ferrite and cementite) to austenite.

Figure 4 compares the thermal expansion of austenitic and duplex stainless steels with the values for carbon steel and concrete taken from EN 1992-1-2 [3]. These stainless steels exhibit greater thermal expansion than carbon steel for all temperatures and do not have the characteristic phase-change plateau at around 750°C. The thermal expansion behaviour of concrete is dependent on the aggregate type used. As shown in Figure 4, this property increases steadily with temperature until around 700 or 800°C (for siliceous or calcareous aggregates, respectively) after which it plateaus and remains constant; this is due to chemical changes in the constituent materials at these temperatures [25].

5. Fire resistant design of structural stainless steel

Unlike carbon steel, stainless steel does not exhibit a clearly defined yield stress at room temperature. Instead, the stress-strain curve is non-linear, with increasing strength accompanied by reducing stiffness (Figure 5). For materials which exhibit these stress-strain characteristics, it is conventional to use the 0.2% proof strength $f_{0.2p}$ as the design strength. Beyond this point, no further strain hardening is considered in traditional design, though it is considered, and systematically harnessed, in the deformation based continuous strength method [26-28]. The non-linear stress-strain characteristics lead to some differences in the structural performance of stainless steel members compared to carbon steel members, which are generally reflected in the design rules set out in EN 1993-1-4 [29].

The fire resistance of structural stainless steel members can be determined using EN 1993-1-2 [30]. The simplified design rules for carbon steel structures can be safely applied to stainless steel in combination with the specific strength and stiffness reduction factors for the grade of stainless steel. The reduction factors are the ratio of strength (or stiffness or strain) at the elevated design temperature to the strength (or stiffness or strain) at room temperature. As mentioned previously, the reduction factors for stainless steel differ quite significantly from those for carbon steel because of the different microstructure and alloying elements. These specific factors for stainless steel are given in Annex C of EN 1993-1-2, where a stress-strain relationship for stainless steel at elevated temperatures is also defined. Since this standard was published, a significant amount of further research has been carried out into the performance of stainless steel in fire [31-38] and more data are available on the performance of a larger number of stainless steels suitable for structural applications. In the next edition of EN 1993-1-2, it is therefore proposed to include eight generic sets of reduction factors which describe the elevated temperature behaviour for a group of stainless steels, instead of a set of reduction factors for each specific grade of stainless steel [39].

When the response of a structural element in fire is considered, larger strains can be tolerated than at room temperature. This reflects the fact that an element is likely to be either repaired or replaced once exposed to fire, meaning large deformations during the fire do not need to be mitigated against. For these reasons, the steel strength at 2% total strain is generally used for fire design in EN 1993. For stainless steel, this can result in a significant increase in strength, as a result of strain hardening. Annex C of EN 1993-1-2 gives an expression (Eq. (1)) for calculating the strength at 2% total strain $f_{y,\theta}$ at a temperature θ from the 0.2% proof stress $f_{0.2p,\theta}$ and ultimate stress $f_{u,\theta}$ at this temperature:

$$f_{y,\theta} = f_{0.2p,\theta} + k_{2\%,\theta}(f_{u,\theta} - f_{0.2p,\theta}) \quad (1)$$

where $k_{2\%,\theta}$ is a factor for calculating $f_{y,\theta}$.

For concrete structures, fire design is covered by EN 1992-1-2 [3]. Reduction factors for the properties of concrete and reinforcing steel are given to account for the degradation of strength and stiffness of the materials with temperature. The degraded material properties are used with temperature-dependent effective depth and width parameters to calculate the resistance at a given temperature, using the same mechanical models as for room temperature design.

EN 1992-1-2 describes the stress-strain relationship of reinforcing steel through the following parameters: the slope of the linear elastic range E_θ, the proportional limit $f_{p,\theta}$ and corresponding strain $\varepsilon_{p,\theta}$, the maximum stress level $f_{y,\theta}$, defined at the strength at 2% strain, and corresponding strain $\varepsilon_{y,\theta} = 0.02$, and the strain at the ultimate tensile stress $\varepsilon_{u,\theta}$. Note that EN 1992-1-2 employs a subscript s in the above symbols to denote steel reinforcement and that the strain at the ultimate tensile stress is denoted $\varepsilon_{st,\theta}$; $\varepsilon_{u,\theta}$ is employed herein for consistency with the notation used for stainless steel in EN 1993-1-2. The stress-strain relationship for reinforcing steel is the same as that given in EN 1993-1-2 for flat structural steel material. Furthermore, the Class N reduction factors for hot rolled carbon steel reinforcing bar are the same as those in EN 1993-1-2 for flat structural steel material. The Class N maximum stress level reduction factors for hot rolled material are greater than or equal to those for cold-worked material for temperatures up to 800°C, while the stiffness reduction factors are greater than or equal to those for cold-worked material at all temperatures.

The purpose of the test programme described in this paper is to investigate whether the same reduction factors for stainless steel flat material can be applied to stainless steel reinforcing bar. The performance of different bar diameters and product forms (plain and ribbed) is also compared.

6. Elevated temperature test programme

An experimental study to determine the elevated temperature material stress-strain properties of stainless steel reinforcing bars was performed in the Structures Laboratory at Imperial College London. A total of 164 elevated temperature material tests were conducted, covering both plain and ribbed reinforcement, austenitic and duplex material and two bar diameters. The tested material was cold-worked to strength class 500. Two testing methods were employed – steady-state (isothermal) and transient-state (anisothermal). In the steady-state tests, the coupons were heated to a target temperature that was then held constant while the coupon was subjected to an increasing axial tensile load until fracture. In the transient-state tests, the coupons were loaded with a target tensile stress that was then held constant while the coupon was heated until fracture. Steady-state tests enable full stress-strain curves, which are suitable for use in analytical and numerical models, to be obtained directly, while transient-state tests more closely mimic realistic fire conditions, i.e. static load followed by increasing temperature. Values were obtained for the following temperature-dependent material properties, where θ is temperature:

- Modulus of elasticity E_θ,
- 0.2% proof strength $f_{0.2p,\theta}$,
- Strength at 2% strain $f_{y,\theta}$,
- Ultimate strength $f_{u,\theta}$,
- Strain at ultimate tensile stress, $\varepsilon_{u,\theta}$, and
- Strain at fracture, $\varepsilon_{f,\theta}$.

These properties are illustrated in Figure 6. From the test results, temperature-dependent reduction factors were calculated for each of the material properties, which are compared later with existing code provisions.

6.1 Test apparatus

Figure 7 shows the test apparatus, which comprised an Instron 750 hydraulic testing machine, an electric furnace capable of heating to temperatures up to 1100°C, a heat control unit with temperature probes which were inserted into the top of furnace, thermocouples attached to the test specimens, rock-wool insulation at either end of the furnace and an extensometer. The extensometer, shown in Figure 8, comprised two clamps fixed to the specimen with pointed bolts, two invar rods, a contact plate and a linear variable differential transducer (LVDT). The machine load, machine displacement, LVDT displacement and thermocouple readings were recorded using the DATASCAN data acquisition equipment and logged using the DSLOG computer package at one second intervals.

6.2 Test specimens

Table 3 summarises the test programme. Each coupon had an overall length of 1000 mm with a gauge length L of 60 mm or 80 mm for the 12 mm and 16 mm bars, respectively. In order to ensure that the coupons failed within the gauge length (thus providing full stress-strain curves up to fracture), the test pieces in this region were narrowed either by a reduction of 1 mm in diameter for the plain round specimens or 0.5 mm on each side for the deformed bars. The extensometer was aligned with the centre of the furnace to ensure that the length of coupon being measured coincided with the region of the furnace at the target test temperature. Standard gauge lengths [40] of $L = 5.65\sqrt{A_o}$, where A_o is the original cross-sectional area of the coupons in the narrowed region, were also marked onto the specimens for the calculation of the fracture strain after testing.

6.3 Testing methods

Two complementary elevated temperature material testing methods were employed in the programme, as described in the following sub-sections. All tests were conducted in accordance with ISO 6892 Parts 1 [40] and 2 [41], following the prescribed heating rates and loading rates.

6.3.1 Steady-state (isothermal) tests

In the steady-state tests, the specimens were heated up to the target temperature at a rate of 10°C/min. A time period of 10 to 15 minutes was allowed after the heating phase for the temperature to settle. The target temperatures ranged from room temperature to 1000°C in increments of 100°C. During the heating phase, the testing machine was set to load control so that the upper jaw of the machine could displace to accommodate the thermal expansion of the specimen, thus ensuring no load was induced. The tensile coupons were then tested until fracture under displacement control at a displacement rate of 0.05 mm/s, in keeping with the strain rates set out in [41]. Typical isothermal stress-strain curves (for the 12 mm diameter grade 1.4307 specimens) are shown in Figure 9 while the reduction factors derived from the results of the steady-state tests are presented in Section 7. The room temperature test results are given in Table 4.

6.3.2 Transient-state (anisothermal) tests

In the transient-state tests, the specimens were first loaded in tension to a particular level and then subjected to increasing temperature until failure. The applied stress levels ranged from 10% to 90% of the ultimate strength at room temperature. While maintaining the loads at these levels, with the testing machine set to load control, the furnace temperature was increased by 10°C/min until failure. The heating rate of 10˚C/min is similar to the rate of temperature increase of protected steelwork during a fire [39]. The actual rate of temperature increase experienced by a reinforcing bar embedded in concrete in typical fire conditions depends on the type of aggregate, cover and thermal gradient through the cross-section and is difficult to measure experimentally, though the high thermal inertia of reinforced concrete structural elements will result in relatively slow rates of temperature increase through the cross-section. Lamond and Pielert [42] report that the maximum temperature to be reached by reinforcing bar in normal weight concrete with 25 mm cover would be around 400-450°C, whereas 50 mm of cover would limit the temperature to around 200°C. Since the strength of the steel decreases with increasing temperature, the higher the applied stress level, the lower the failure temperature. The results of the transient-state tests are presented in Section 7.

The displacement readings from the extensometer comprised components relating to the mechanical tensile strain of the coupons, the thermal strain of the coupons and also some thermal strains associated with the extensometer apparatus itself. For the steady-state tests, once the target temperature was achieved, the extensometer reading was zeroed and thus only the mechanical strain was measured. For the transient-state tests, however, both mechanical and thermal strains arise with increasing temperature. To isolate the thermal strains, extensometer readings were taken during the heating phase of an unloaded coupon up to 1000°C. The resulting thermal strains were then deducted from the total temperature-strain plots to give only the strains induced from the effect of the applied load.

By examining the full set of transient-state temperature-strain curves, of which there is one at each applied stress level, stress-strain curves can be derived by extracting strains corresponding to a specific temperature from each curve, and plotting these against the respective applied stresses, as demonstrated in Figure 10, resulting in a set of isothermal stress-strain curves. For higher temperatures, for example at θ_2 in Figure 10, fewer data points are available since for transient-state tests performed at the higher applied stress levels (f_3 in the example) the failure temperature is lower than the temperature in question.

7. Test results and recommendations

7.1 Reduction factors

The results of the tests (i.e. the derived reduction factors) are presented in Figures 11 to 22 for the austenitic stainless steel (grades 1.4307 and 1.4311) reinforcing bars and Figures 23 to 34 for the duplex stainless steel (grades 1.4162 and 1.4362) reinforcement. The derived reduction factors, which may be used in simplified fire design methods, are compared with the reduction factors given in EN 1992-1-2 for cold-worked carbon steel reinforcement and the reduction factors set out by Gardner et al. [39] for different groups of austenitic

and duplex stainless steels. Note that EN 1992-1-2 does not provide reduction factors for 0.2% proof strength for carbon steel reinforcement, so comparisons are made against the proportional limit reduction factors for this property. The three groups of austenitic stainless steels defined by Gardner et al. [39] are: austenitic I (1.4301, 1.4318 and 1.4818), austenitic II (1:4401/4 and 1.4541) for more highly alloyed or stabilised grades and austenitic III (1.4571), this stabilised grade being treated separately due to its superior elevated temperature performance. The two austenitic stainless steel grades tested herein are most closely aligned to the austenitic I group, and comparisons are therefore made with the reduction factors proposed for this group. The two groups of duplex stainless steel [39] are duplex I (1.4362) and, with higher nitrogen content, duplex II (1.4462 and 1.4162). The results for the two duplex grades tested herein are compared with the reduction factors for their corresponding group. The reduction factors proposed by Gardner et al. [39] will be recommended for inclusion in the next revision of EN 1993-1-2. The following comparisons and observations are made:

- No consistent differences were noted between the results of isothermal and anisothermal tests or between the reduction factors of the 12 mm and 16 mm diameter bars. Similarly, the results for the plain and ribbed bars follow a comparable pattern. Therefore, in the assessment of reduction factors, all data are given equal weighting.

- The reduction factors derived from the test results for the 0.2% proof strength ($k_{0.2p} = f_{0.2p,\theta}/f_{0.2p}$) are plotted in Figures 11 and 12 for the austenitic grades and Figure 23 and 24 for the duplex grades with the reduction factors of Gardner et al. [39] derived for flat stainless steel material, and also the proportional limit reduction factors for carbon steel cold-worked reinforcement given in EN 1992-1-2 [3]. All the results from the isothermal tests lie on or above the recommended stainless steel reduction factor curves. However, many of the anisothermal test results fall below the recommended curves, particularly at 800°C and above. This may be partly attributed to the difficulty in obtaining reliable values for 0.2% proof strengths from anisothermal tests at these very high temperatures, but also reflects the findings of previous research on cold-formed stainless steel sections [43], which showed that strength enhancements derived from cold-work are lost at 800°C and above. It was therefore recommended in [39] that, for 800°C and above, the elevated temperature 0.2% proof strength should be based on the recommended reduction factors, but multiplied by the room temperature 0.2% proof strength of the annealed material (i.e. removing the benefit of cold-work). Presented in an alternative fashion, the room temperature properties are fixed, but the recommended 0.2% proof strength reduction factors are multiplied by the ratio of the annealed to the cold-worked 0.2% proof strength for 800°C and above. The same recommendation is made herein for reinforcement, though it should be noted that reinforcing steel, embedded in concrete, is unlikely to experience such high temperatures.

- The reduction factors derived from the test results for the ultimate strength ($k_u = f_{u,\theta}/f_u$) – see Figures 13 and 14 for the austenitic grades and Figures 25 and 26 for the duplex grades – are plotted with the recommended stainless steel reduction factors from [39] and those for carbon steel cold-worked reinforcement in EN 1992-1-2, noting in the latter case that reduction factors for ultimate strength

are the same as those for the strength at 2% strain (referred to as yield strength and denoted $f_{sy,\theta}$ in EN 1992-1-2). The test results are generally well represented by the recommended stainless steel reduction factors [39], including at the very high temperatures. Compared to the 0.2% proof strength, the influence of cold-work is far less pronounced on the ultimate strength; it is therefore recommended that no adjustment is needed to the reduction factors to account for this.

- The test results for the $k_{2\%,\theta}$ factor are plotted in Figures 15 and 16 for the austenitic grades and Figures 27 and 28 for the duplex grades with the values given in [39]. Note that the $k_{2\%,\theta}$ factors define the strength at 2% strain as a proportion of the difference between the 0.2% proof strength and the ultimate strength. Therefore, when the values of the 0.2% proof strength and the ultimate strength are close, experimental data for the $k_{2\%,\theta}$ factor can become rather scattered, as is the case herein, and sensitive to the degree of cold-work to which the material has been subjected. However, in such circumstances, since the strength at 2% strain in already closely bound (by the 0.2% proof strength and ultimate strength), the influence of the $k_{2\%,\theta}$ factor is very small. It is recommended that the proposed values for the $k_{2\%,\theta}$ factor based on flat material [39] may also be applied to stainless steel reinforcement.

- The reduction factors derived from the isothermal test results for the modulus of elasticity ($k_E = E_\theta/E$) are plotted in Figures 17 and 18 for the austenitic grades and Figures 29 and 30 for the duplex grades with the values for stainless steel given in EN 1993-1-2 and the values for carbon steel cold-worked bar given in EN 1992-1-2. The test results are generally well represented by the Eurocode reduction factors for stainless steel up to about 600°C, though at higher temperatures, the experimental reduction factors are generally below those given in the code. This, as well as the high degree of scatter, has also been observed in previous studies [39, 43]. It is important to note that, as previously stated, the temperature of steel reinforcement in a fire is unlikely to ever be greater than 400-450°C due to the presence of surrounding concrete [42]. Nevertheless, further research is needed in this area, and it is recommended herein that consideration is given to having different reduction factors for modulus of elasticity for the different families of stainless steel, rather than the single set of reduction factors currently given in EN 1993-1-2.

- The reduction factors derived from the test results for the ultimate strain ($k_{\varepsilon u} = \varepsilon_{u,\theta}/\varepsilon_u$), where ε_u is the ultimate strain at room temperature, are plotted in Figures 19 and 20 for the austenitic grades and Figures 31 and 32 for the duplex grades with the values for stainless steel given in EN 1993-1-2 and the recommendations made by Chen and Young [44]. Note that there are no existing recommendations for grade 1.4362 stainless steel (Figure 32). The EN 1993-1-2 reduction factors and the Chen and Young recommendations generally follow the same trend as the test data, which is reducing ductility with temperature until about 800°C, followed by plateauing or rising values. The test ultimate strains are however consistently below those predicted by EN 1993-1-2, and hence revised reduction factors, presented in Table 5 and shown in Figures 19, 20, 31 and 32 are recommended. The proposals are based on the mean of the obtained data, and also considering the

results of Chen and Young [44] as an additional data set, since their recommendations were based on single data sets for grades 1.4301 and 1.4162 stainless steel. For the grade 1.4362 material, reduction factors have been proposed in the absence of existing values. The proposed reduction factors are assumed to be representative of their respective groups (austenitic I, duplex I and duplex II).

- The reduction factors derived from the test results for the fracture strain ($k_{\varepsilon f} = \varepsilon_{f,\theta}/\varepsilon_f$) where ε_f is the fracture strain at room temperature, are plotted in Figures 21 and 22 for the austenitic grades and Figures 33 and 34 for the duplex grades. The consistent trend of the test results is for the fracture strain to initially reduce below the room temperature value for temperatures up to about 800°C, beyond which higher fracture strains are observed. In the absence of reduction factors recommended in codes or the literature, those values set out in Table 5, based on the mean of the obtained test data, are proposed. Note that the same reduction factors are proposed for both of the examined duplex grades.

Overall, it is proposed that the existing reduction factors derived for flat material [39] for 0.2% proof strength, ultimate strength and strength and 2% strain may be safely applied to stainless steel reinforcement up to strength class 500. For ultimate strain, revised reduction factors have been proposed since the obtained data were consistently below those recommended in EN 1993-1-2, while for fracture strain, reduction factors are proposed in the absence of existing provisions. For Young's modulus reduction factors, no new reduction factors have been proposed, though it is recommended that further work is carried out on this topic and that distinction be made between the different families of stainless steel in future revisions of EN 1993-1-2.

7.2 Material stress-strain relationship

The basic form of the stress-strain curves obtained for the tested stainless steel reinforcement (see Figure 9) generally follows that observed for flat material at both room and elevated temperature. It is therefore proposed that the two-stage Ramberg-Osgood stress-strain model, which has been extensively validated for representing the behaviour of flat stainless steel material, may also be used to describe the stress-strain response of stainless steel reinforcement, in applications such as advanced analytical and numerical modelling.

7.2.1 Room temperature stress-strain curves

The two-stage Ramberg-Osgood expression [45, 46] adopted in EN 1993-1-4 [29] for the description of the stress-strain response of stainless steel at room temperature is an extension of the original single stage expression developed by Ramberg and Osgood [1] and modified by Hill [2]. In the two-stage model, the original Ramberg-Osgood expression, given by Eq. (2), is used to describe the stress-strain behaviour up to the 0.2% proof strength $f_{0.2p}$. In Eq. (2), n is the strain hardening exponent whose value depends on the grade of stainless steel [29, 47, 48].

$$\varepsilon = \frac{\sigma}{E} + 0.002\left(\frac{\sigma}{f_{0.2p}}\right)^{n} \quad \text{for } \sigma \leq f_{0.2p} \tag{2}$$

The second part of the two-stage model, given by Eq. (3), applies for stresses above the 0.2% proof strength, up to the ultimate tensile strength. In Eq. (3), $E_{0.2}$ is the tangent modulus at the 0.2% proof stress, $\varepsilon_{0.2}$ is the total strain at the 0.2% proof stress and m is the strain hardening exponent for the second part of the two-stage model.

$$\varepsilon = \frac{\sigma - f_{0.2p}}{E_{0.2}} + \varepsilon_u\left(\frac{\sigma - f_{0.2p}}{f_u - f_{0.2p}}\right)^{m} + \varepsilon_{0.2} \qquad \text{for } f_{0.2p} < \sigma < f_u \tag{3}$$

As an alternative to Eq. (3), the second part of the two-stage model may be defined on the basis of a Ramberg-Osgood curve passing through the 1% proof stress $f_{1.0p}$, as given by Eq. (4), where $\varepsilon_{1.0}$ is the total strain at the 1% proof stress and $n_{0.2,1.0}$ is the strain hardening exponent for the second part of the two-stage model described by Eq. (4).

$$\varepsilon = \frac{\sigma - f_{0.2p}}{E_{0.2}} + \left(\varepsilon_{1.0} - \varepsilon_{0.2} - \frac{f_{1.0p} - f_{0.2}}{E_{0.2}}\right)\left(\frac{\sigma - f_{0.2p}}{f_{1.0p} - f_{0.2p}}\right)^{n_{0.2,1.0}} + \varepsilon_{0.2} \qquad \text{for } f_{0.2p} < \sigma < f_u \tag{4}$$

Although very accurate representations of the stress-strain response of stainless steel up to the ultimate stress can be achieved using either Eq. (3) or Eq. (4), Eq. (4) would generally be slightly more accurate at higher strains since the curve passes, approximately [48], through the ultimate stress/strain point, while Eq. (4) would generally be slightly more accurate at lower strains since the curve passes through the 1% proof stress. Eq. (3) is therefore considered to be more suitable for modelling scenarios where very high strain would be expected (e.g. connections) while Eq. (4) may be more suitable for modelling stainless steel structural members. Additionally, a three-stage model, which utilises Eq. (4) up to 2% strain, followed by a linear relationship has been proposed [50].

Typical comparisons between the measured room temperature stress-strain curves on stainless steel reinforcement (for 1.4162D12 material) from the present study and the two (Eqs (2) and (3) and Eqs (2) and (4)) two-stage Ramberg-Osgood models described above are shown in Figure 35. Both models may be seen to provide an excellent representation of the experimental curves and are thus deemed suitable for the description of the stress-strain response of stainless steel reinforcement. For the data shown in Figure 35, the maximum absolute error between the measured test stress-strain curve and the Ramberg-Osgood models is about 20 N/mm^2 for both Eqs (2) and (3) and Eqs (2) and (4), though this corresponds to a point on the early part of the stress-strain curve where stress is varying rapidly with strain. The mean absolute error over the full range of data is 3.3 N/mm^2 for Eqs (2) and (3) and 4.8 N/mm^2 for Eqs (2) and (4). Average values for the strain hardening parameters n, m and $n_{0.2,1.0}$ obtained from the tests performed in the present study are reported in Table 6.

7.2.2 Elevated temperature stress-strain curves

For the representation of stainless steel stress-strain curves at elevated temperatures, the two-stage Ramberg-Osgood concept has also been shown to be applicable [39, 44]. For stresses up to the elevated temperature 0.2% proof strength $f_{0.2p,\theta}$, the original Ramberg-Osgood, but based on elevated temperature properties, where n_θ is the strain hardening exponent at temperature θ [39, 44].

$$\varepsilon = \frac{\sigma}{E_\theta} + 0.002\left(\frac{\sigma}{f_{0.2p,\theta}}\right)^{n_\theta} \qquad \text{for } \sigma \le f_{0.2p,\theta} \tag{5}$$

For the second part of the two-stage model, Gardner et al. [39] proposed Eq. (6), which passes through the elevated temperature strength at 2% strain $f_{y,\theta}$. This point was chosen since the strength at 2% strain is generally employed in structural fire design, and reduction factors for its determination are readily available. In Eq. (6), $E_{0.2,\theta}$ is the tangent modulus at the elevated temperature 0.2% proof stress, $\varepsilon_{0.2,\theta}$ and $\varepsilon_{1.0,\theta}$ are the total strains at the elevated temperature 0.2% and 1.0% proof strengths, respectively, and $n_{\theta,2}$ [39] is the elevated temperature strain hardening exponent for the second part of the two-stage model described by Eq. (6).

$$\varepsilon = \frac{\sigma - f_{0.2p,\theta}}{E_{0.2,\theta}} + \left(0.02 - \varepsilon_{0.2,\theta} - \frac{f_{y,\theta} - f_{0.2p,\theta}}{E_{0.2,\theta}}\right)\left(\frac{\sigma - f_{0.2p,\theta}}{f_{y,\theta} - f_{0.2p,\theta}}\right)^{n_{\theta,2}} + \varepsilon_{0.2,\theta} \quad \text{for } f_{0.2p,\theta} < \sigma < f_{u,\theta} \tag{6}$$

Analogous to Eq. (3), the second part of the two-stage Ramberg-Osgood model can also be formulated to pass through the ultimate stress at elevated temperature $f_{u,\theta}$, as given by Eq. (7) [44], where m_θ [44] is the elevated temperature strain hardening exponent for the second part of the two-stage model described by Eq. (6).

$$\varepsilon = \frac{\sigma - f_{0.2p,\theta}}{E_{0.2,\theta}} + \varepsilon_{u,\theta}\left(\frac{\sigma - f_{0.2p,\theta}}{f_{u,\theta} - f_{0.2p,\theta}}\right)^{m_\theta} + \varepsilon_{0.2,\theta} \qquad \text{for } f_{0.2p,\theta} < \sigma < f_{u,\theta} \tag{7}$$

As at room temperature, both two-stage Ramberg-Osgood models have been shown to be capable of providing an accurate representation of elevated temperatures stainless steel stress-strain curves [39,44], with Eq. (6) being slightly more precise at lower strains and Eq. (7) being slightly more precise at higher strains. Comparisons of both models with measured elevated stress-strain curves (for 1.4162D12 material) from the present study are shown in Figure 36. For the data shown in Figure 36, the average (for the seven elevated temperatures) maximum absolute error between the measured test stress-strain curve and the Ramberg-Osgood models is about 20 N/mm^2 for both Eqs (2) and (3) and Eqs (2) and (4), though again, as for the room temperature comparisons, this corresponds to points on the early part of the stress-strain curves where stress is varying rapidly with strain. The average (for the seven elevated temperatures) mean absolute error over the full ranges of data is 3.7 N/mm^2 for Eqs (2) and (3) and 4.4 N/mm^2 for Eqs (2) and (4). Average

values for the elevated temperature strain hardening parameters n_θ, m_θ and $n_{\theta,2}$ obtained from the tests performed in the present study are reported in Table 6.

8. Conclusions

The use of stainless steel reinforcement in place of carbon steel reinforcement is becoming an increasingly common means of improving the durability of reinforced concrete structures. In this paper, previous applications are outlined and factors affecting the specification of stainless steel reinforcement are described. Consideration was then given to the elevated temperature material properties of stainless steel reinforcing bars, which is important for structural fire design. A total of 164 elevated temperature material tests (isothermal and anisothermal) were conducted, covering both plain and ribbed reinforcement, austenitic and duplex material and two bar diameters. No consistent differences were observed between the results of isothermal and anisothermal tests or between the reduction factors of the 12 mm and 16 mm diameter bars or the plain and ribbed bars. The obtained test results showed that the reduction factors for 0.2% proof strength, strength at 2% strain and ultimate strength derived for stainless steel plate and strip can also be applied to stainless steel reinforcing bar. Revised reduction factors for ultimate strain and fracture strain at elevated temperatures have been proposed. The ability of two-stage Ramberg-Osgood expressions to capture accurately the stress-strain response of stainless steel reinforcement at both room temperature and elevated temperatures is also demonstrated.

Acknowledgements

The authors gratefully acknowledge the support of Outokumpu who supplied the test specimens, and the assistance of Mr Ge Yin and Mr Gordon Herbert in the laboratory testing programme.

References

[1] Euro Inox/SCI. Design manual for structural stainless steel. Third ed. Building series, vol. 3. Euro Inox and the Steel Construction Institute; 2006.

[2] Gardner L, Ng KT. Temperature development in structural stainless steel sections exposed to fire. Fire Safety Journal, 2006;41(3):185-203.

[3] EN 1992-1-2. Eurocode 2: Design of concrete structures. Part 1.2 General rules. Structural fire design. CEN; 2004.

[4] Garlock M, Paya-Zaforteza I, Kodur V, Gu L. Fire hazard in bridges: Review, assessment and repair strategies. Engineering Structures 2012;35:89-98

[5] Barkley T, G. Strasburg G. Bridge Rebuilt on the Fast Track, U.S. Department of Transportation Federal Highway Administration. Available from: https://www.fhwa.dot.gov/publications/publicroads/02sep/05.cfm. Updated July 4, 2011, Accessed Oct 20, 2015.

[6] Giuliani L, Crosti C, Gentili F. Vulnerability of bridges to fire. In: Proceedings of the 6th International Conference on Bridge Maintenance, Safety and Management: 2012 July 8-12; Stresa, Lake Maggiore, Italy. CRC Press.

[7] The Concrete Society. Guidance on the use of stainless steel reinforcement, Concrete Society Technical Report No. 51. 1998.

[8] Nickel Institute. Stainless rebar: past present and future. Nickel Magazine 2014 March;29(1):4. Available at: http://nickelinstitute.org/en/NickelMagazine/MagazineHome/AllArchives/2014/Volume29-1/InUseStainlessRebar.aspx. Accessed 10th November 2015.

[9] Gedge G. The use of stainless steel reinforcement in bridges. The British Stainless Steel Association, 2003.

[10] The Highways Agency. Design manual for roads and bridges, Volume 1 Highway structures: Approval procedures and general design Section 3: General design, Part 8 - BA 57/01 - Design for durability. 2001.

[11] Marsh BK. Stainless steel reinforcement – The use of predictive models in specifying selective use of stainless steel reinforcement. Ove Arup & Partners Ltd; 2009.

[12] Virginia Department of Transportation. Corrosion resistant reinforcing steels (CRR). Virginia: Structure and Bridge Division; 2012 August. Report No. IIM-S&B-81.5.

[13] Azom. Synopsis of research on the performance of MMFX reinforcing steel in concrete structures. 2013 August. Available from: http://www.azom.com/article.aspx?ArticleID=9852. Accessed Oct 20, 2015.

[14] Abbasi A, Hogg PJ. Prediction of the failure time of glass fiber reinforced plastic reinforced concrete beams under fire conditions. Journal of Composites for Construction 2005;9(5):450-457.

[15] BS 6744. Stainless steel bars for the reinforcement of and use in concrete. Requirements and test methods. British Standards Institution; 2001.

[16] ASTM A955 / A955M-15. Standard specification for deformed and plain stainless-steel bars for concrete reinforcement. ASTM International, West Conshohocken, PA, USA; 2015.

[17] EN 10080. Steel for the reinforcement of concrete, Weldable reinforcing steel, General. British Standards Institution; 2005.

[18] ASTM A615 / A615M-15a. Standard specification for deformed and plain carbon-steel bars for concrete reinforcement. ASTM International, West Conshohocken, PA, USA; 2015.

[19] EN 10088-1. Stainless steels Part 1: List of stainless steels. British Standards Institution; 2014.

[20] ASTM A276 / A276M-15. Standard specification for stainless steel bars and shapes. ASTM International, West Conshohocken, PA, USA; 2015.

[21] Gedge G. Structural uses of stainless steel — buildings and civil engineering. Journal of Constructional Steel Research 2008;64(9): 1194-1198.

[22] Gardner L. Aesthetics, economics and design of stainless steel structures. Advanced Steel Construction. 2008; 4(2): 113-122.

[23] Theofanous M and Gardner L. (2010). Experimental and numerical studies of lean duplex stainless steel beams. Journal of Constructional Steel Research. 2010; 66(6):816-825.

[24] Huang Y and Young B. Tests of pin-ended cold-formed lean duplex stainless steel columns. Journal of Constructional Steel Research. 2013; 82: 203-215.

[25] Wang YC, Burgess IW, Wald F, Gillie M. Performance-based fire engineering of structures. CRC Press; 2012.

[26] Theofanous M, Prospert T, Knobloch M and Gardner L. The continuous strength method for steel cross-section design at elevated temperatures. Thin-Walled Structures. 2016; 98: 94-102.

[27] Afshan S. and Gardner L. The continuous strength method for structural stainless steel design. Thin-Walled Structures. 2013; 68: 42-49.

[28] Buchanan C, Gardner L and Liew A. The continuous strength method for the design of circular hollow sections. Journal of Constructional Steel Research. 2016; 118: 207-216.

[29] EN 1993-1-4. Eurocode 3: Design of steel structures. Part 1-4: General rules. Supplementary rules for stainless steel. CEN; 2006.

[30] EN 1993-1-2. Eurocode 3. Design of steel structures. Part 1-2: General rules. Structural fire design. CEN; 2005.

[31] Ng KT and Gardner L. Buckling of stainless steel columns and beams in fire. Engineering Structures. 2007; 29(5): 717-730.

[32] Gardner L. Stainless steel structures in fire. Proceedings of the Institution of Civil Engineers - Structures and Buildings. 2007; 160(3): 129-138.

[33] Fan S, Ding X, Sun W, Zhang L, Liu M. Experimental investigation on fire resistance of stainless steel columns with square hollow section. Thin-Walled Structures, 2016; 98A: 196-211.

[34] Tondini N, Rossi B and Franssen JM. Experimental investigation on ferritic stainless steel columns in fire, Fire Safety Journal, 2013; 62C: 238-248.

[35] Han LH, Chen F, Liao FY, Tao Z and Uy B. Fire performance of concrete filled stainless steel tubular columns, Engineering Structures, 2013; 56: 165-181.

[36] Lopes N, Vila Real P, Simões da Silva L, Franssen JM. Numerical analysis of stainless steel beam-columns in case of fire, Fire Safety Journal, 2012; 50: 35-50.

[37] Cai Y and Young B. Bearing factors of cold-formed stainless steel double shear bolted connections at elevated temperatures, Thin-Walled Structures, 2016; 98A: 212-229.

[38] Huang Y and Young B. Stress–strain relationship of cold-formed lean duplex stainless steel at elevated temperatures, Journal of Constructional Steel Research, 2014; 92: 103-113.

[39] Gardner L, Insausti A, Ng KT, Ashraf M. Elevated temperature material properties of stainless steel alloys. Journal of Constructional Steel Research 2010; 66:634-647.

[40] ISO 6892-1. Metallic materials. Tensile testing Part 1: Method of test at room temperature; International Standards Organisation; 2009.

[41] ISO 6892-2. Metallic materials. Tensile testing Part 2: Method of test at elevated temperature; International Standards Organisation; 2011.

[42] Lamond JF, Pielert JH. Significance of tests and properties of concrete and concrete-making materials, STP169D. ASTM International; 2006.

[43] Ala-Outinen T. Fire resistance of austenitic stainless steel Polarit 725 (EN 1.4301) and Polarit 761 (EN 1.4571). VTT research notes 1760. Espoo (Finland). 1996.

[44] Chen J, Young B. Stress-strain curves for stainless steel at elevated temperatures. Engineering Structures 2006:28 (2):229-239.

[45] Mirambell E and Real E. On the calculation of deflections in structural stainless steel beams: an experimental and numerical investigation. Journal of Constructional Steel Research, 2000; 54(4): 109-133.

[46] Rasmussen KJR. Full-range stress–strain curves for stainless steel alloys. Journal of Constructional Steel Research, 2003; 59(1): 47-61.

[47] Afshan S, Rossi B, Gardner L. Strength enhancements in cold-formed structural sections – Part I: Material testing. Journal of Constructional Steel Research, 2013; 83: 177–188.

[48] Arrayago I, Real E and Gardner L. Description of stress-strain curves for stainless steel alloys. Materials and Design, 2015; 87: 540-552.

[49] Gardner L and Ashraf M. Structural design for non-linear metallic materials. Engineering Structures, 2006; 28(6): 926-934.

[50] Quach WM, Teng JG and Chung KF. Three-Stage Full-Range Stress-Strain Model for Stainless Steels. Journal of Structural Engineering ASCE, 2008; 134(9): 1518-1527.

Table 1 Equivalent designation of the stainless steels in the test programme

EN 10088 designation	Popular designation	UNS designation	Strength grade
1.4307	304L	S30403	500
1.4311	304LN	S30453	500
1.4162	LDX 2101®	S32101	500
1.4362	2304	S32304	500

Table 2 Guidance on use of stainless steel reinforcement for different service conditions from BS 6744 [15]

Stainless steel grade	Service condition			
	For structures or components with either a long design life, or which are inaccessible for future maintenance	For structures or components exposed to chloride contamination with no relaxation in durability design (e.g. concrete cover, quality or water proofing treatment requirements)	Reinforcement bridging joints, or penetrating the concrete surface and also subject to chloride contamination (e.g. dowel bars or holding down bolts)	Structures subject to chloride contamination where reductions in normal durability requirements are proposed (e.g. reduced cover, concrete quality or omission of water proofing treatment)
1.4301	1	1	4	3
1.4162	1	1	4	3
1.4362	2	2	1	1

Key
1 – Appropriate choice for corrosion resistance and cost.
2 – Over-specification of corrosion resistance for the application.
3 – May be suitable in some instances: specialist advice should be obtained.
4 – Unsuitable for the application.

Table 3 Summary of test specimens

Specimen ID	Stainless steel grade	Bar type	Diameter (mm)	No. of steady-state tests	No. of transient-state tests
4307R12	1.4307	Plain round	12	10	9
4162R12	1.4162	Plain round	12	10	9
4307R16	1.4307	Plain round	16	10	9
4362R16	1.4362	Plain round	16	10	9
4311D12	1.4311	Ribbed	12	10	5
4162D12	1.4162	Ribbed	12	10	8
4162D16	1.4162	Ribbed	16	10	7
4311D16	1.4311	Ribbed	16	10	9
4362D16	1.4362	Ribbed	16	10	9

Table 4 Summary of the mechanical properties of the test bars at room temperature

Specimen	Product form	$f_{0.2p}$ (MPa)	f_u (MPa)	E (MPa)	ε_u (%)	ε_f (%)
4307R12	Plain round bars	562	796	210200	30.7	39.9
4162R12		805	964	208700	2.9	18.8
4307R16		537	751	211100	31.4	42.4
4362R16		760	860	197500	3.0	22.0
4311D12	Ribbed bars	480	764	202600	38.6	48.3
4162D12		682	874	199100	20.4	32.4
4162D16		646	844	195200	22.5	32.9
4311D16		528	717	199900	32.9	47.9
4362D16		608	834	171400	11.5	35.1

Table 5 Proposed reduction factors for ultimate strain and fracture strain for stainless steel

Reduction factor	Group	Temperature (°C)										
		20	100	200	300	400	500	600	700	800	900	1000
Ultimate strain reduction factor $k_{\varepsilon u}$	Austenitic I	1.00	0.56	0.42	0.42	0.42	0.42	0.33	0.24	0.15	0.15	0.20
	Duplex I	1.00	1.00	1.00	1.00	1.00	1.00	1.00	0.80	0.60	0.40	0.40
	Duplex II	1.00	0.87	0.74	0.74	0.74	0.74	0.74	0.44	0.14	0.14	0.14
Fracture strain reduction factor $k_{\varepsilon f}$	Austenitic I	1.00	0.78	0.50	0.50	0.50	0.50	0.50	0.50	0.50	1.00	1.50
	Duplex I and II	1.00	0.90	0.78	0.78	0.78	0.78	0.78	0.78	0.78	2.40	4.00

Table 6 Average values for the strain hardening parameters obtained from the tests performed in the present study

	n	m	$n_{0.2,1.0}$	n_{θ}	m_{θ}	$n_{\theta,2}$
Austenitic	4.7	4.8	4.8	7.9	7.1	5.6
Duplex	5.3	5.0	4.4	6.3	7.9	6.5

Figure 1 Progreso Pier, Mexico – the pier in the background was constructed in 1940 and used stainless steel reinforcing bar whereas the pier in the foreground was constructed in 1969 and used carbon steel reinforcing bar (Courtesy of the Nickel Institute)

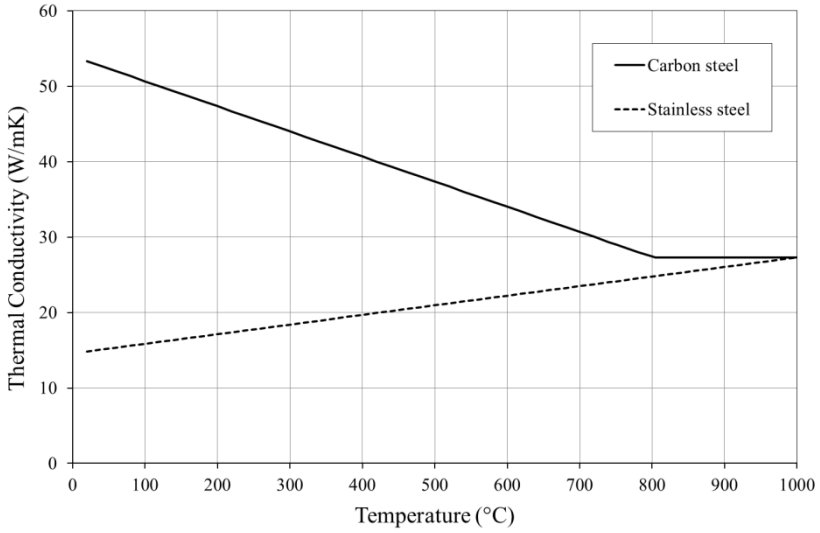

Figure 2 Comparison of thermal conductivity of stainless steel and carbon steel

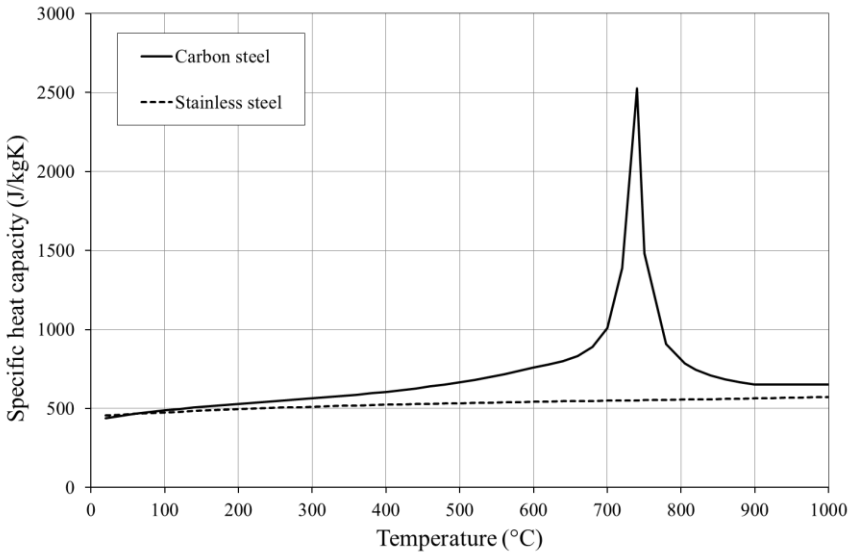

Figure 3 Comparison of specific heat capacity of stainless steel and carbon steel

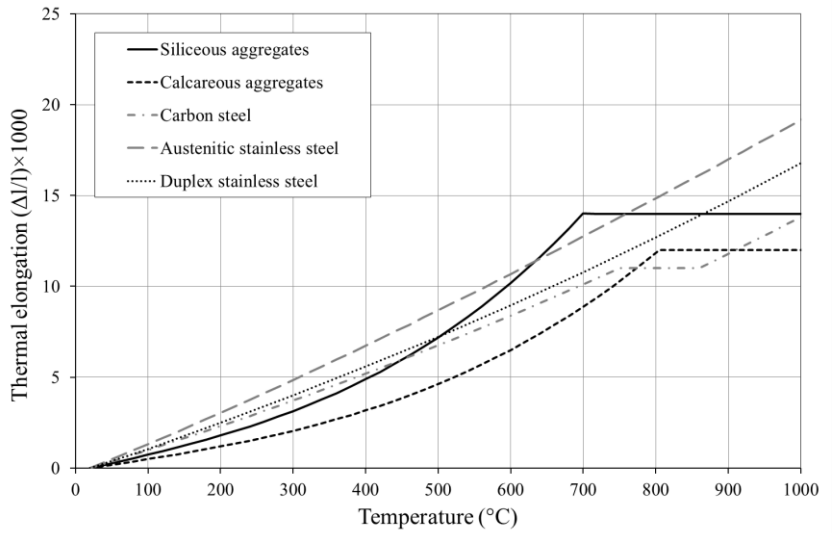

Figure 4 Comparison of thermal expansion of stainless and carbon steel

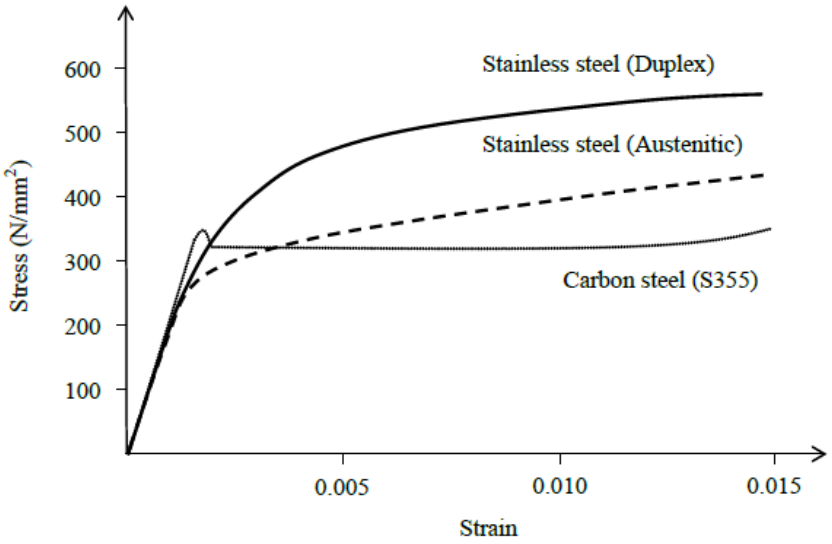

Figure 5 Typical stress-strain curves for stainless steel and carbon steel

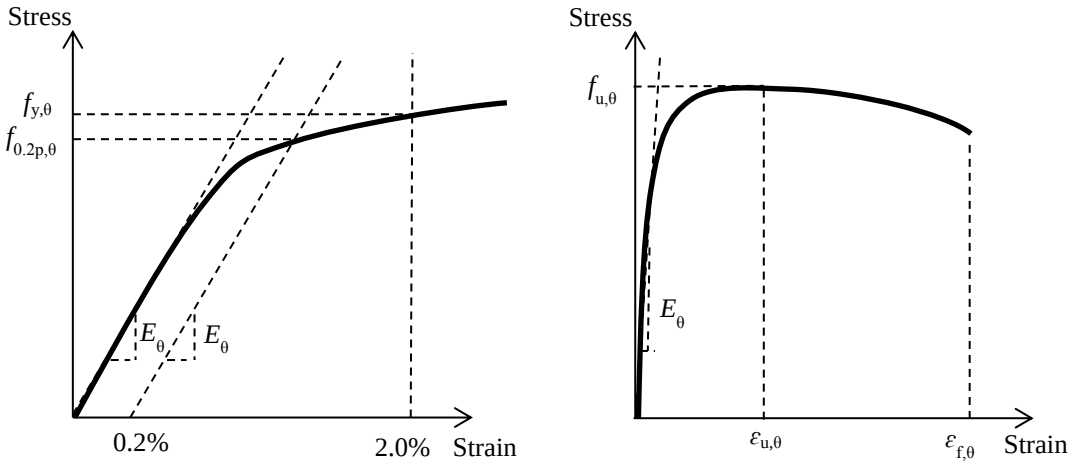

(a) Initial portion of stress-strain curve (b) Full stress-strain curve

Figure 6 Definition of measured elevated temperature material properties

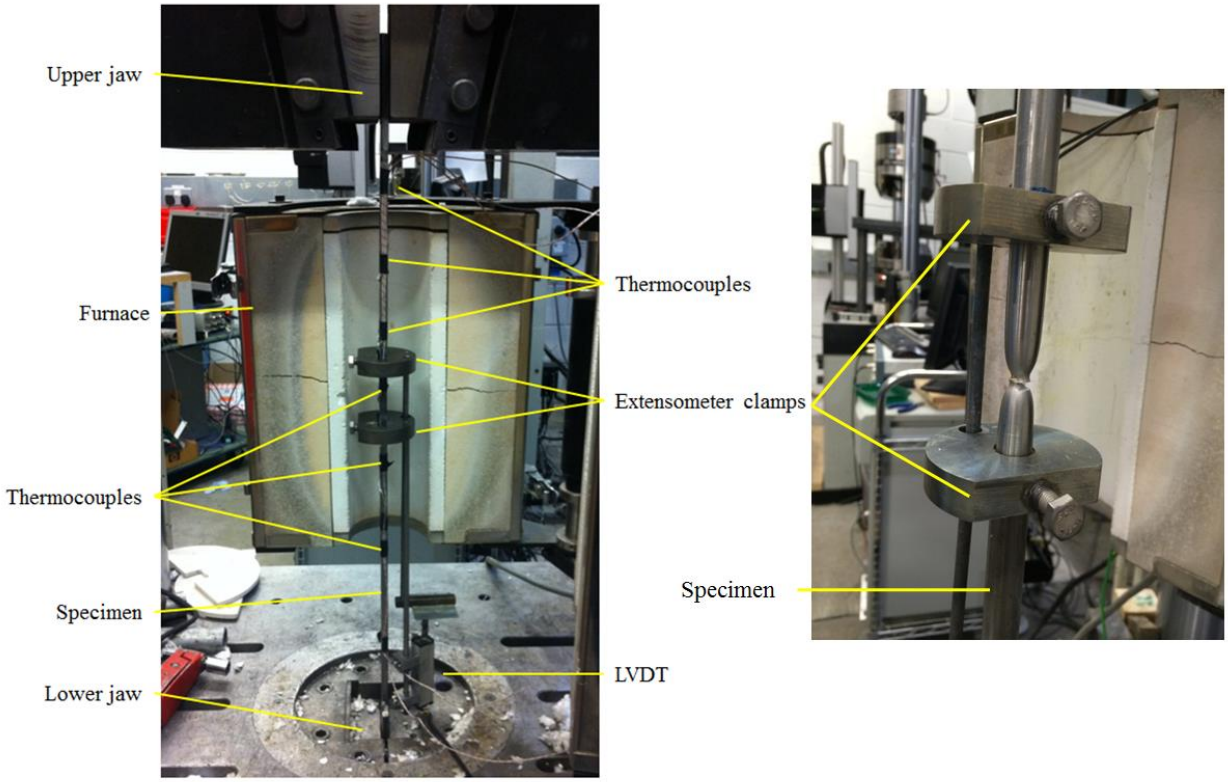

Figure 7 Apparatus for elevated temperature tests

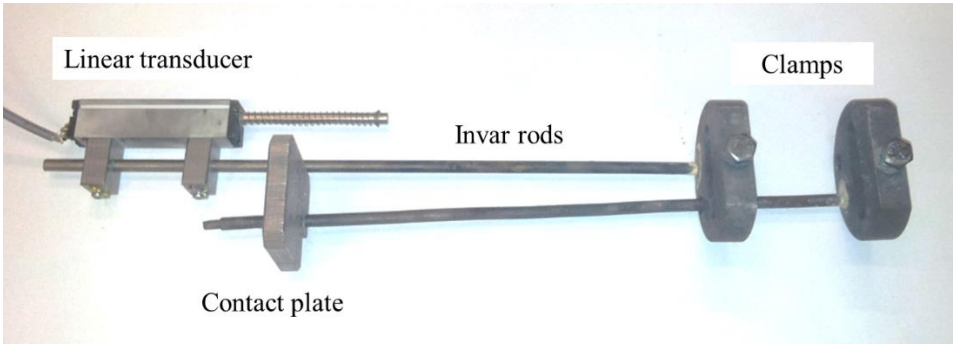

Figure 8 Extensometer components used to record strain

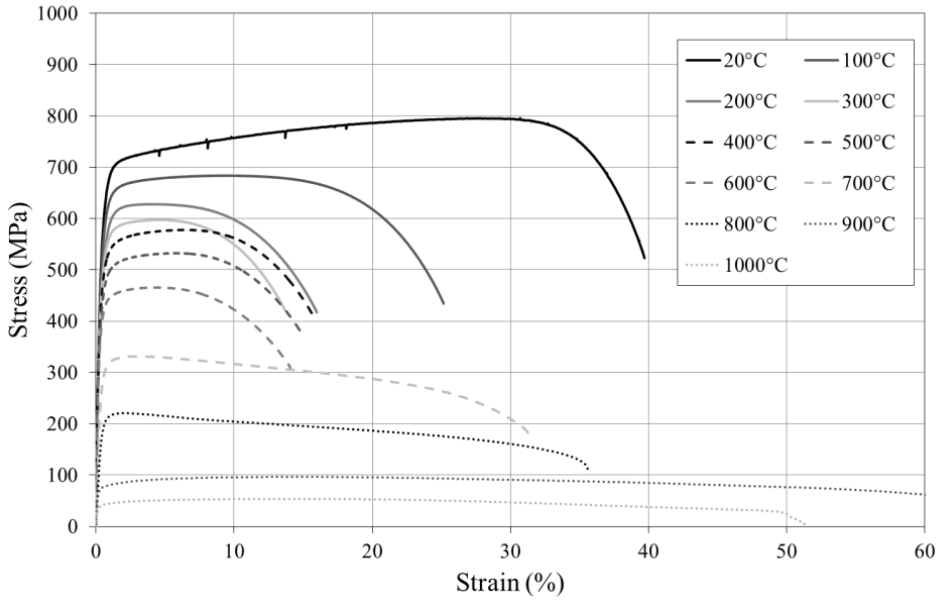

Figure 9 Isothermal stress-strain curves for grade 1.4307 austenitic stainless steel bars with a diameter of 12 mm

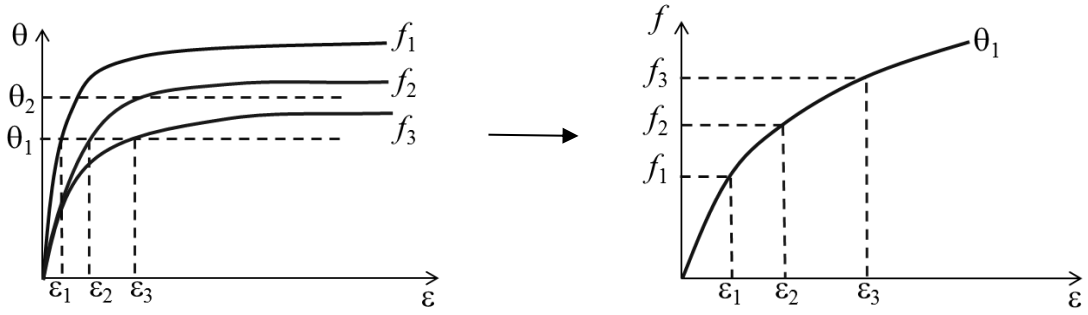

Figure 10 Derivation of isothermal stress-strain curves from transient-state test temperature-strain data.

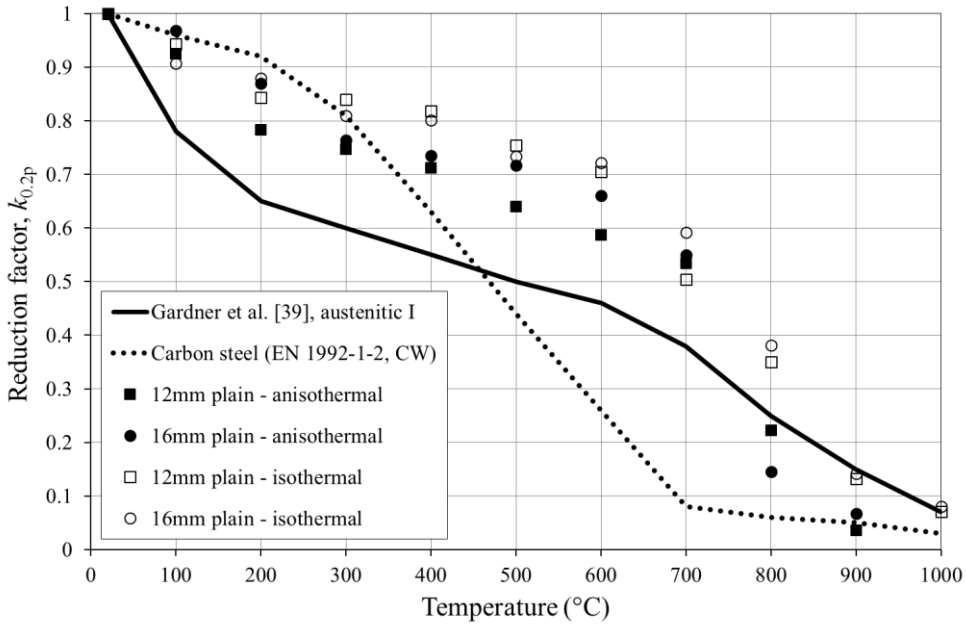

Figure 11 Reduction factors for 0.2% proof strength for austenitic grade 1.4307 stainless steel, compared with recommendations of Gardner et al. [39] for stainless steel (austenitic group I) and EN 1992-1-2 for carbon steel

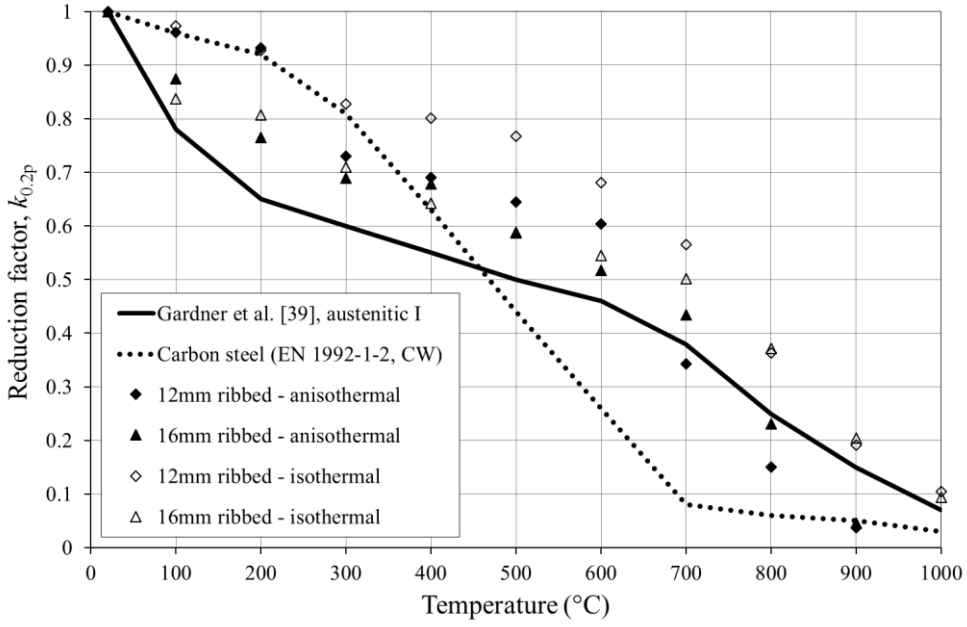

Figure 12 Reduction factors for 0.2% proof strength for austenitic grade 1.4311 stainless steel, compared with recommendations of Gardner et al. [39] for stainless steel (austenitic group I) and EN 1992-1-2 for carbon steel

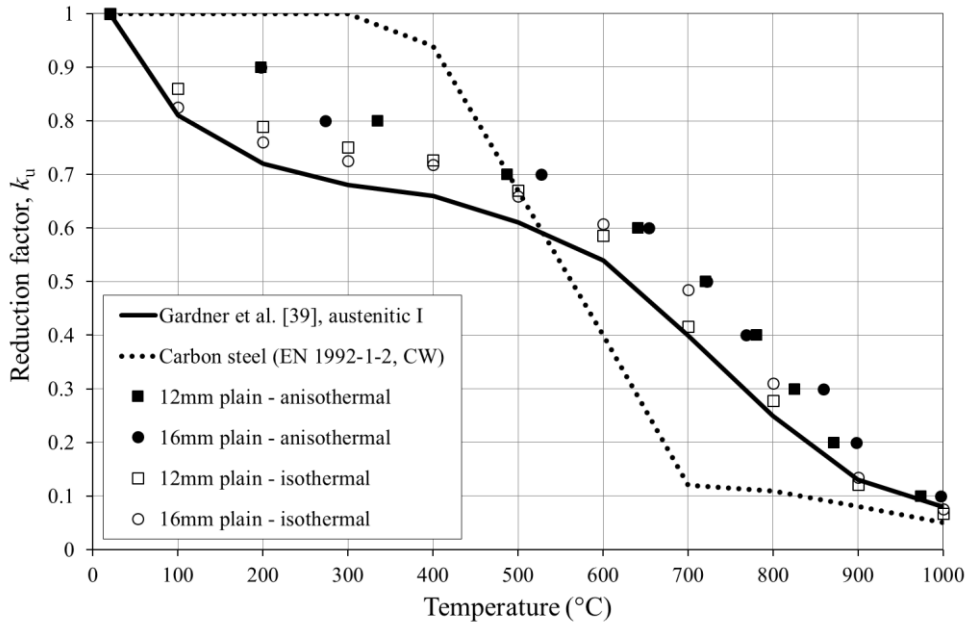

Figure 13 Reduction factors for ultimate tensile strength for austenitic grade 1.4307 stainless steel, compared with recommendations of Gardner et al. [39] for stainless steel (austenitic group I) and EN 1992-1-2 for carbon steel

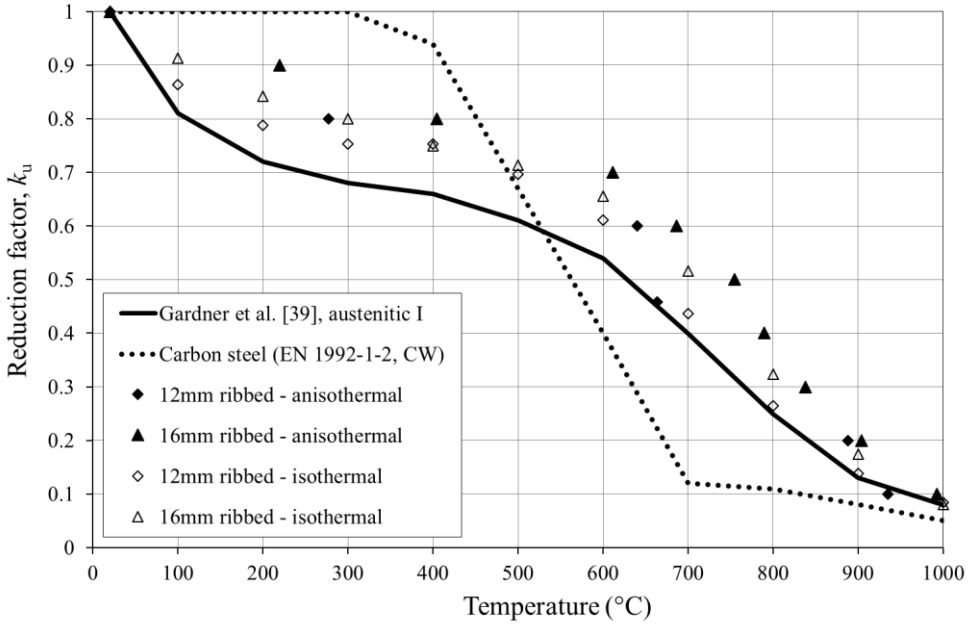

Figure 14 Reduction factors for ultimate tensile strength for austenitic grade 1.4311 stainless steel, compared with recommendations of Gardner et al. [39] for stainless steel (austenitic group I) and EN 1992-1-2 for carbon steel

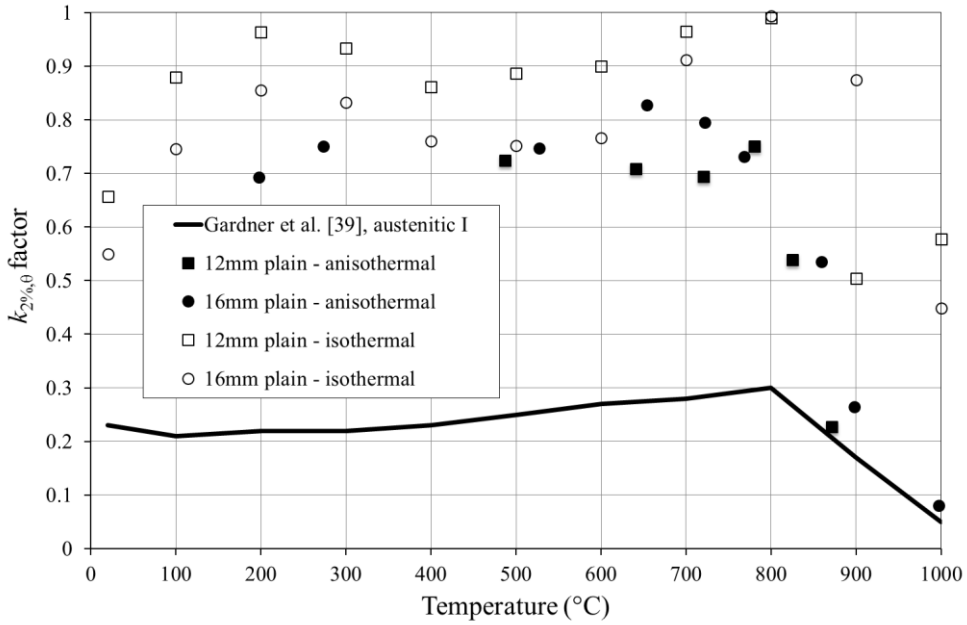

Figure 15 $k_{2\%,\theta}$ factors for determining the strength at 2% strain for austenitic grade 1.4307 stainless steel, compared with recommendations of Gardner et al. [39] for stainless steel (austenitic group I)

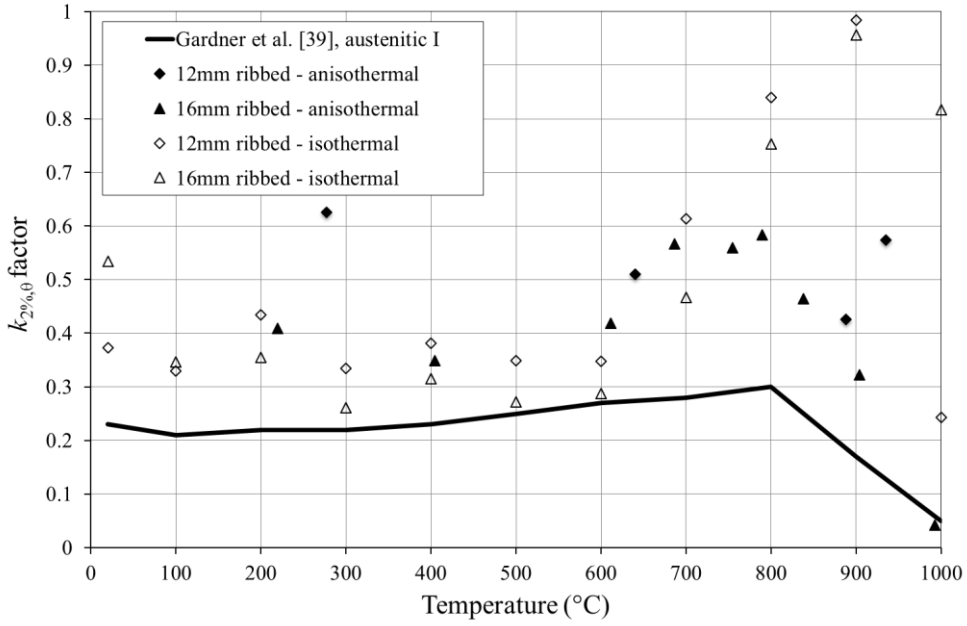

Figure 16 $k_{2\%,\theta}$ factors for determining the strength at 2% strain for austenitic grade 1.4311 stainless steel, compared with recommendations of Gardner et al. [39] for stainless steel (austenitic group I)

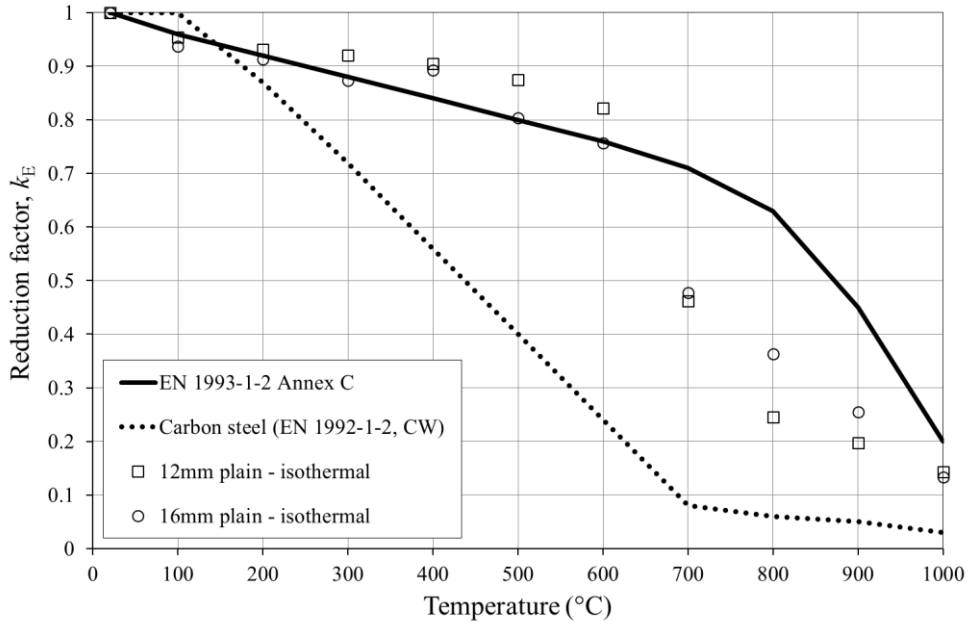

Figure 17 Reduction factors for modulus of elasticity for austenitic grade 1.4307 stainless steel, compared with values given in EN 1993-1-2 Annex C for stainless steel and EN 1992-1-2 for carbon steel

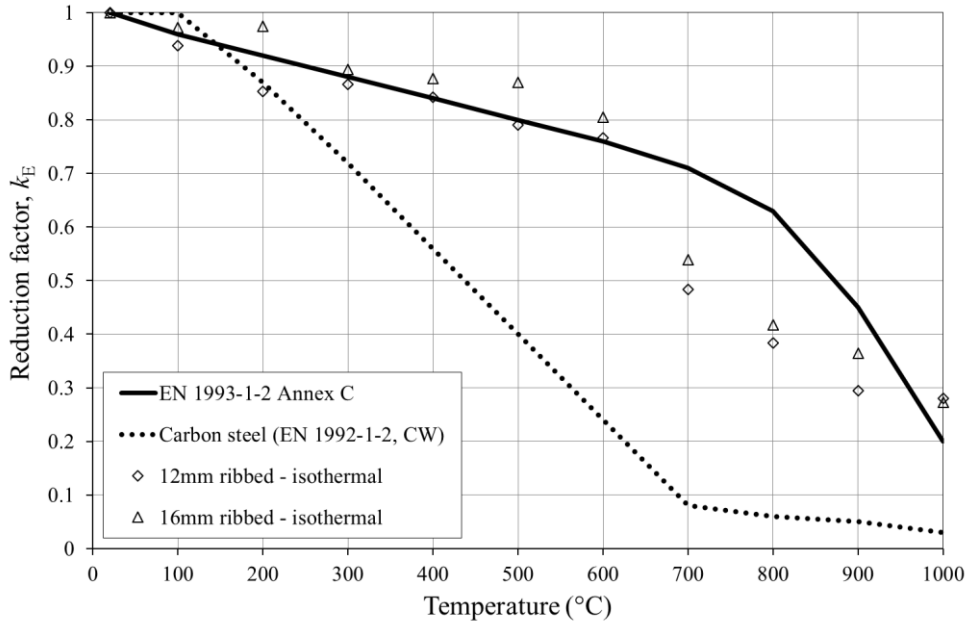

Figure 18 Reduction factors for modulus of elasticity for austenitic grade 1.4311 stainless steel, compared with values given in EN 1993-1-2 Annex C for stainless steel and EN 1992-1-2 for carbon steel

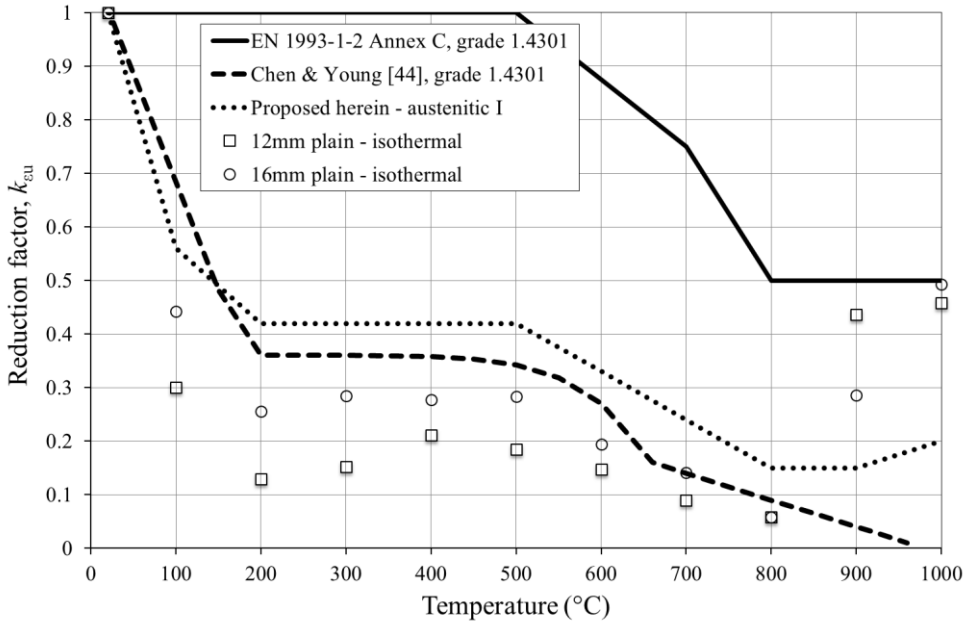

Figure 19 Reduction factors for ultimate strain for austenitic grade 1.4307 stainless steel, compared with values given in EN 1993-1-2 Annex C and recommended by Chen and Young [44] for grade 1.4301 stainless steel, together with proposed values for austenitic group I

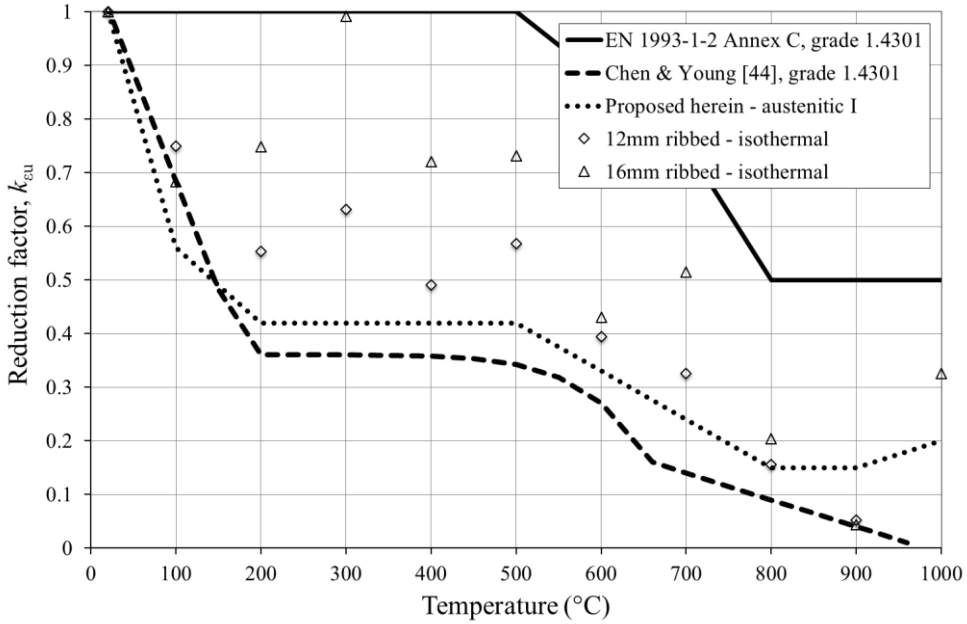

Figure 20 Reduction factors for ultimate strain for austenitic grade 1.4311 stainless steel, compared with values given in EN 1993-1-2 Annex C and recommended by Chen and Young [44] for grade 1.4301 stainless steel, together with proposed values for austenitic group I

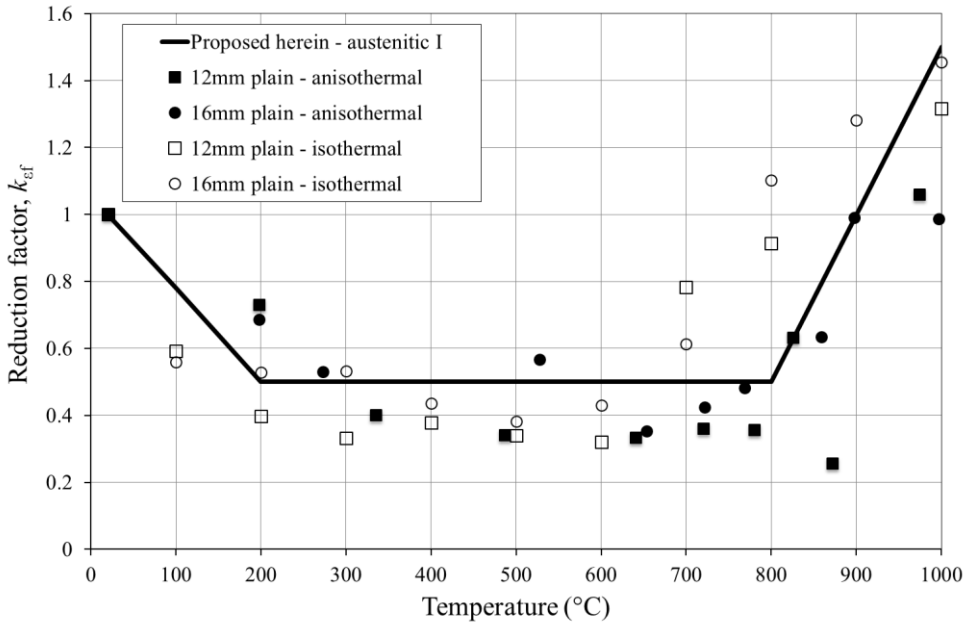

Figure 21 Reduction factors for fracture strain for austenitic grade 1.4307 stainless steel, together with proposed values for austenitic group I

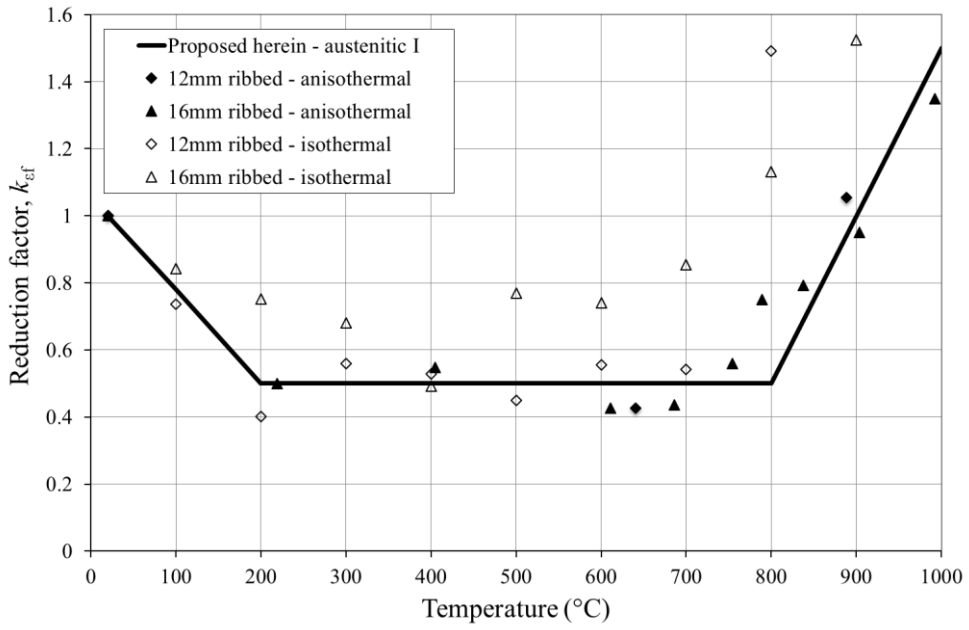

Figure 22 Reduction factors for fracture strain for austenitic grade 1.4311 stainless steel, together with proposed values for austenitic group I

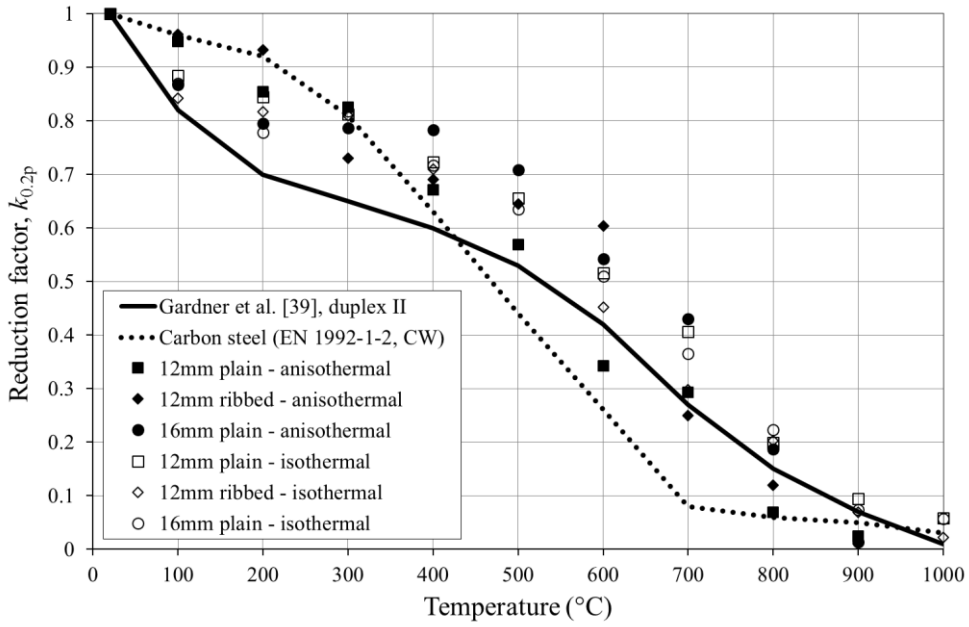

Figure 23 Reduction factors for 0.2% proof strength for duplex grade 1.4162 stainless steel, compared with recommendations of Gardner et al. [39] for stainless steel (duplex group II) and EN 1992-1-2 for carbon steel

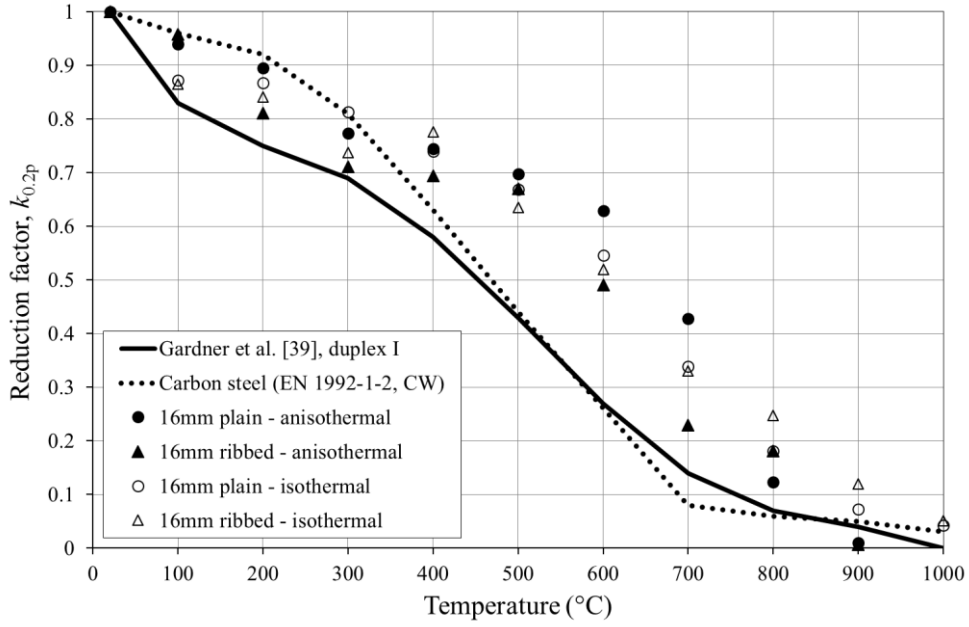

Figure 24 Reduction factors for 0.2% proof strength for duplex grade 1.4362 stainless steel, compared with recommendations of Gardner et al. [39] for stainless steel (duplex group I) and EN 1992-1-2 for carbon steel

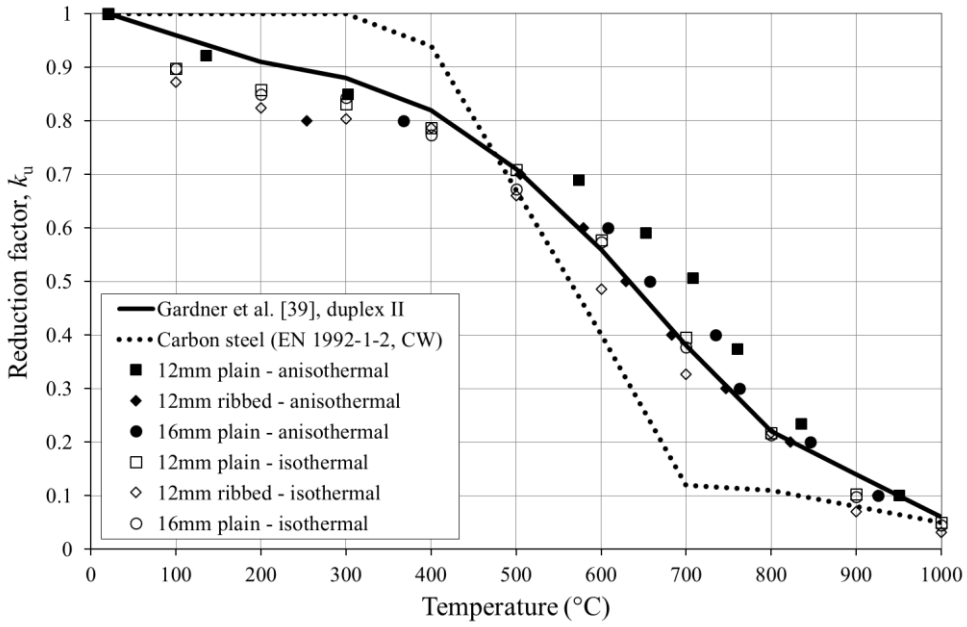

Figure 25 Reduction factors for ultimate tensile strength for duplex grade 1.4162 stainless steel, compared with recommendations of Gardner et al. [39] for stainless steel (duplex group II) and EN 1992-1-2 for carbon steel

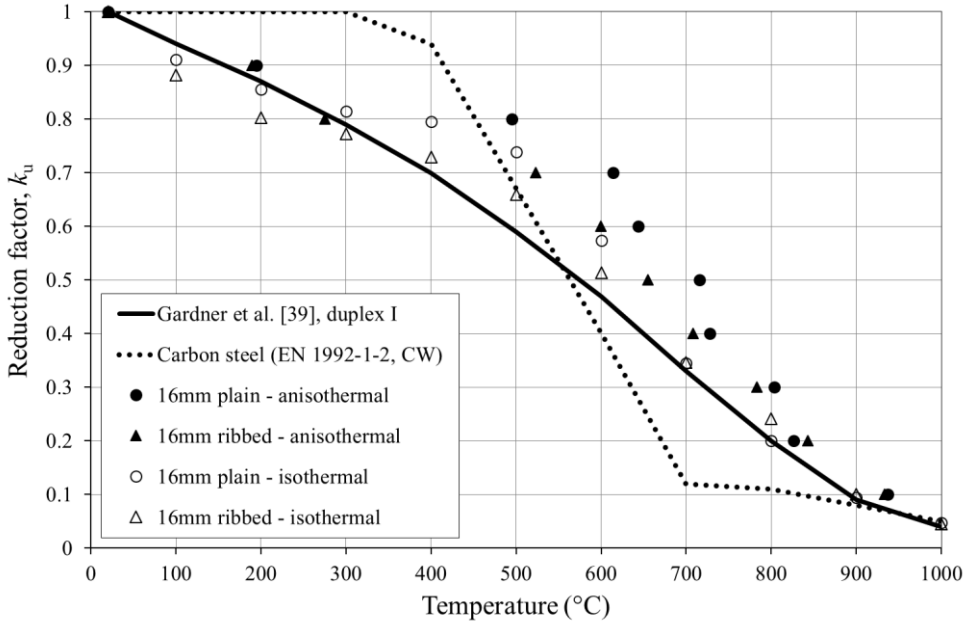

Figure 26 Reduction factors for ultimate tensile strength for duplex grade 1.4362 stainless steel, compared with recommendations of Gardner et al. [39] for stainless steel (duplex group I) and EN 1992-1-2 for carbon steel

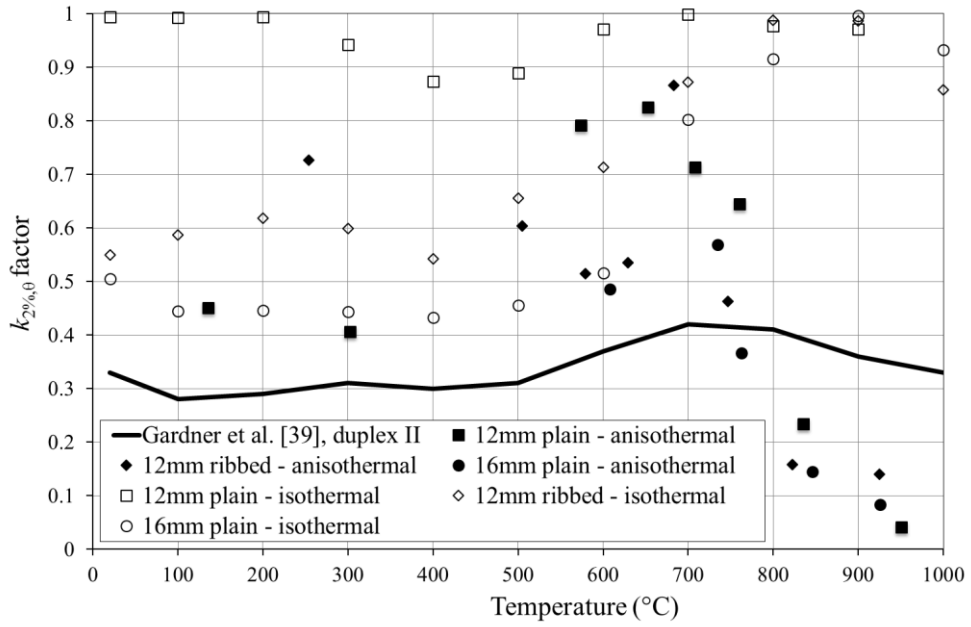

Figure 27 $k_{2\%,\theta}$ factors for determining the strength at 2% strain for duplex grade 1.4162 stainless steel, compared with recommendations of Gardner et al. [39] for stainless steel (duplex group II)

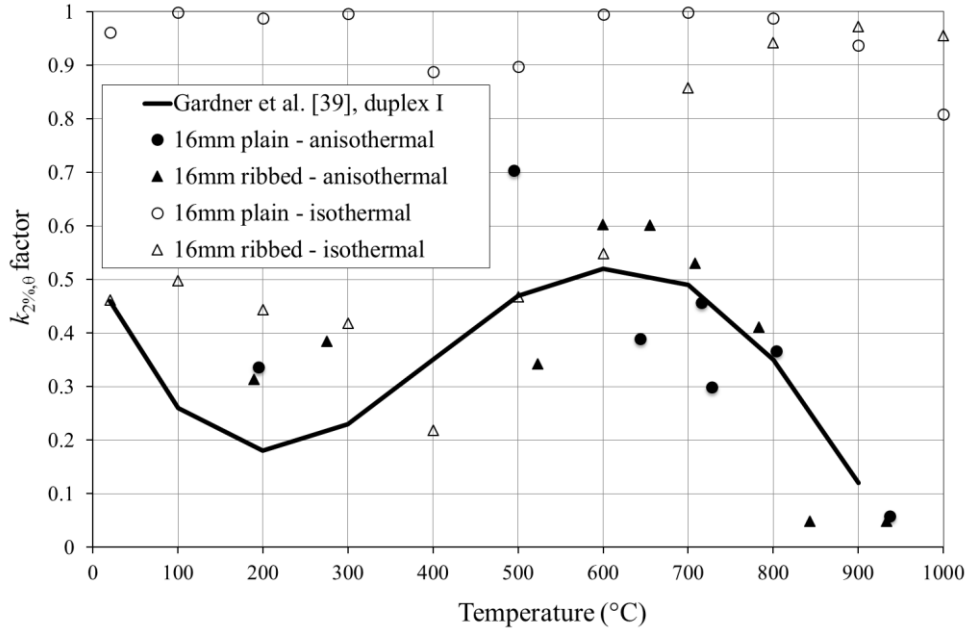

Figure 28 $k_{2\%,\theta}$ factors for determining the strength at 2% strain for duplex grade 1.4362 stainless steel, compared with recommendations of Gardner et al. [39] for stainless steel (duplex group I)

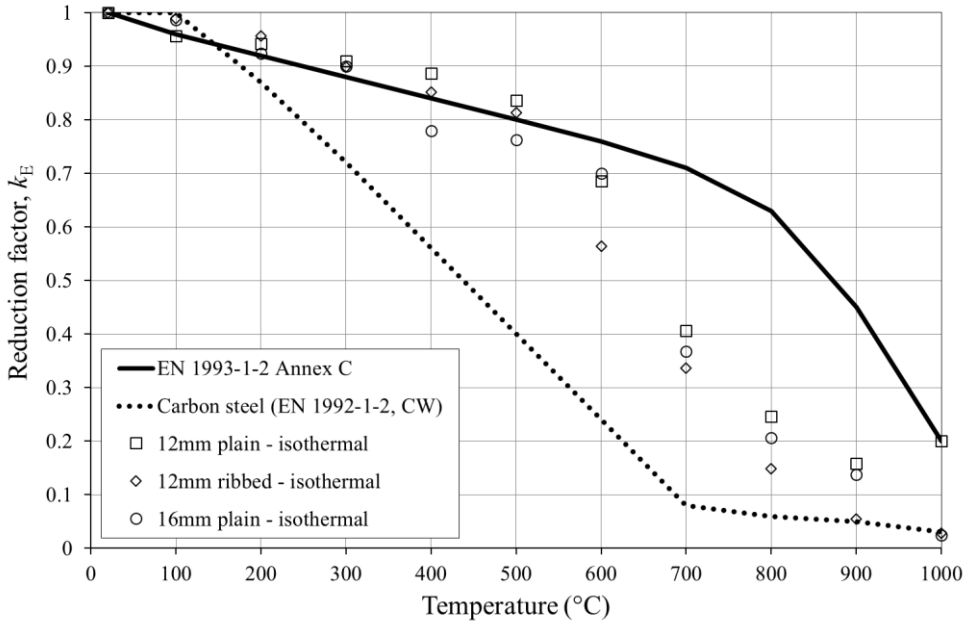

Figure 29 Reduction factors for modulus of elasticity for austenitic grade 1.4162 stainless steel, compared with values given in EN 1993-1-2 Annex C for stainless steel and EN 1992-1-2 for carbon steel

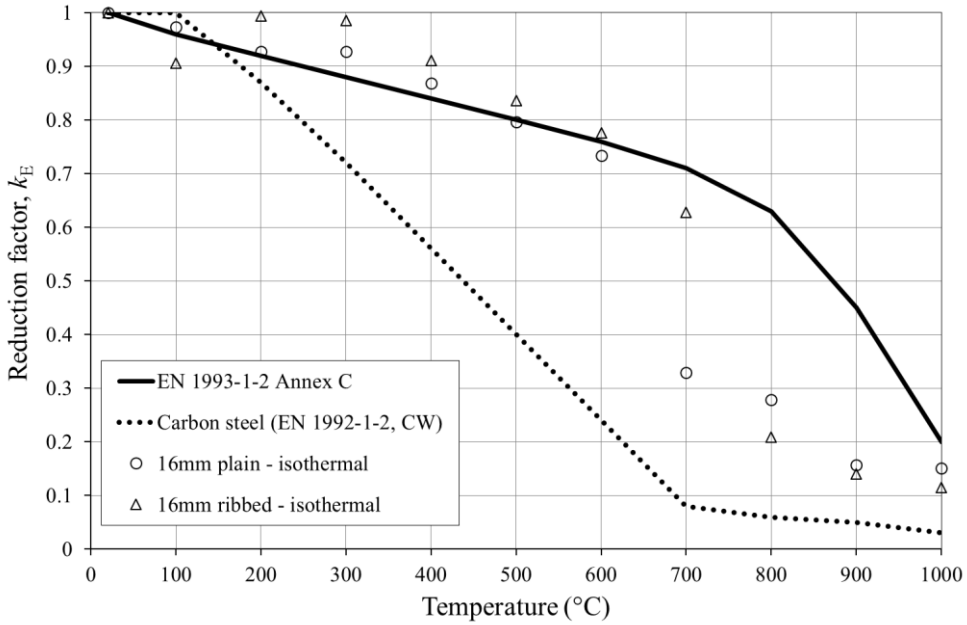

Figure 30 Reduction factors for modulus of elasticity for austenitic grade 1.4362 stainless steel, compared with values given in EN 1993-1-2 Annex C for stainless steel and EN 1992-1-2 for carbon steel

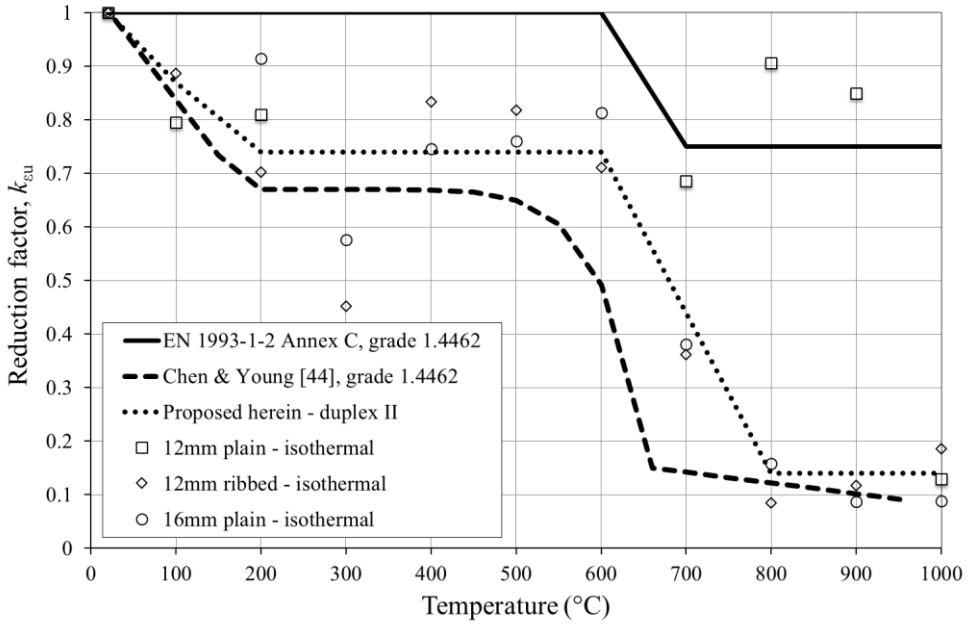

Figure 31 Reduction factors for ultimate strain for duplex grade 1.4162 stainless steel, compared with values given in EN 1993-1-2 Annex C and recommended by Chen and Young [44] for grade 1.4462 stainless steel, together with proposed values for duplex group II

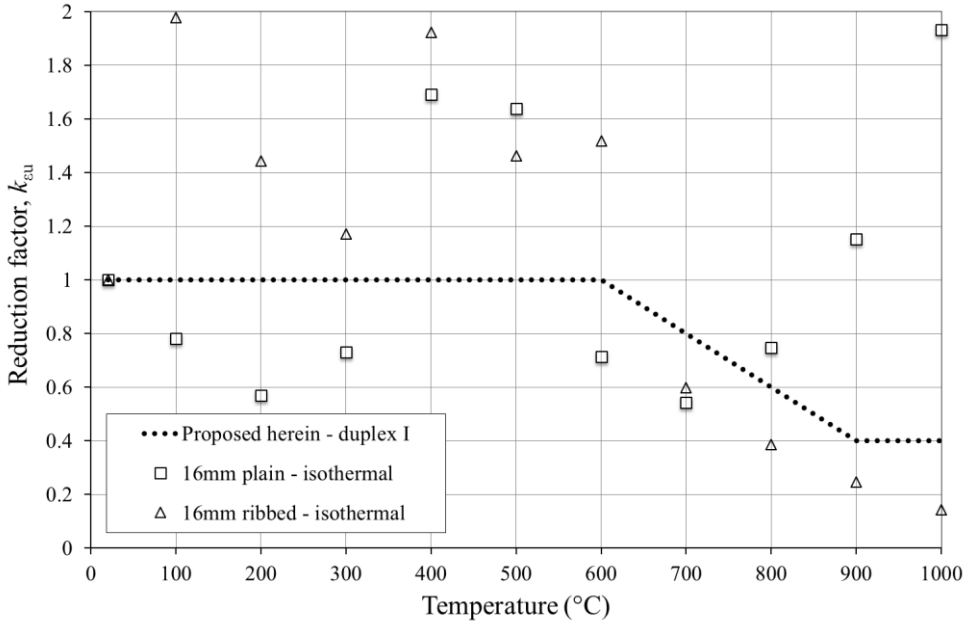

Figure 32 Reduction factors for ultimate strain for duplex grade 1.4362 stainless steel, together with proposed values for duplex group I

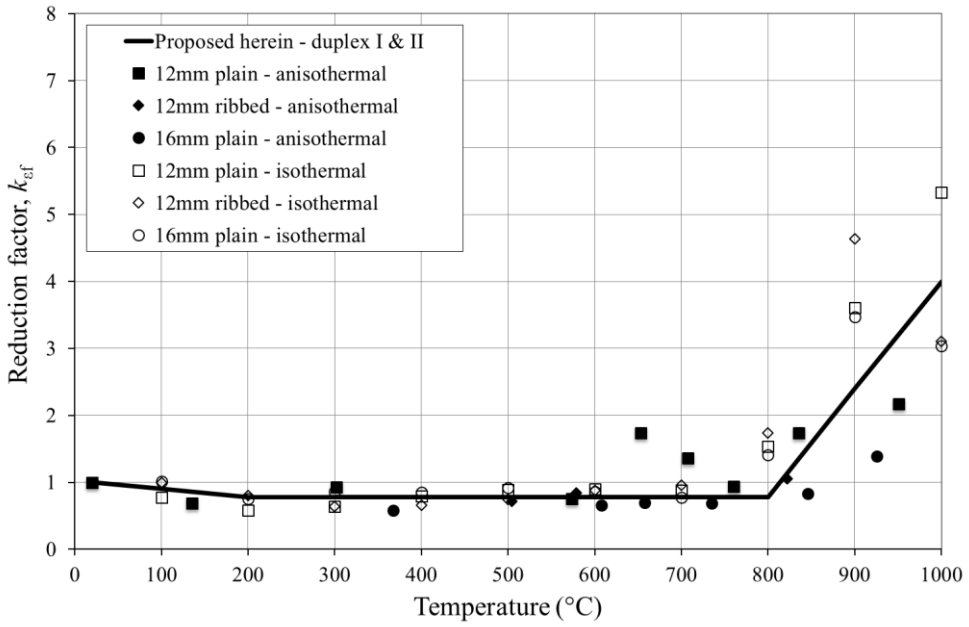

Figure 33 Reduction factors for fracture strain for duplex grade 1.4162 stainless steel, together with proposed values for duplex groups I and II

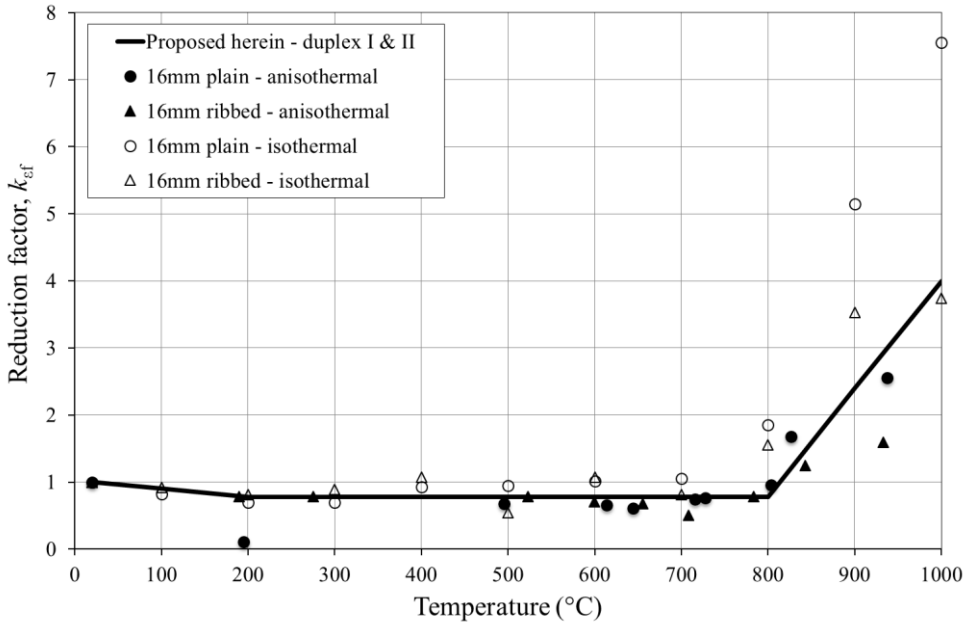

Figure 34 Reduction factors for fracture strain for duplex grade 1.4362 stainless steel, together with proposed values for duplex groups I and II

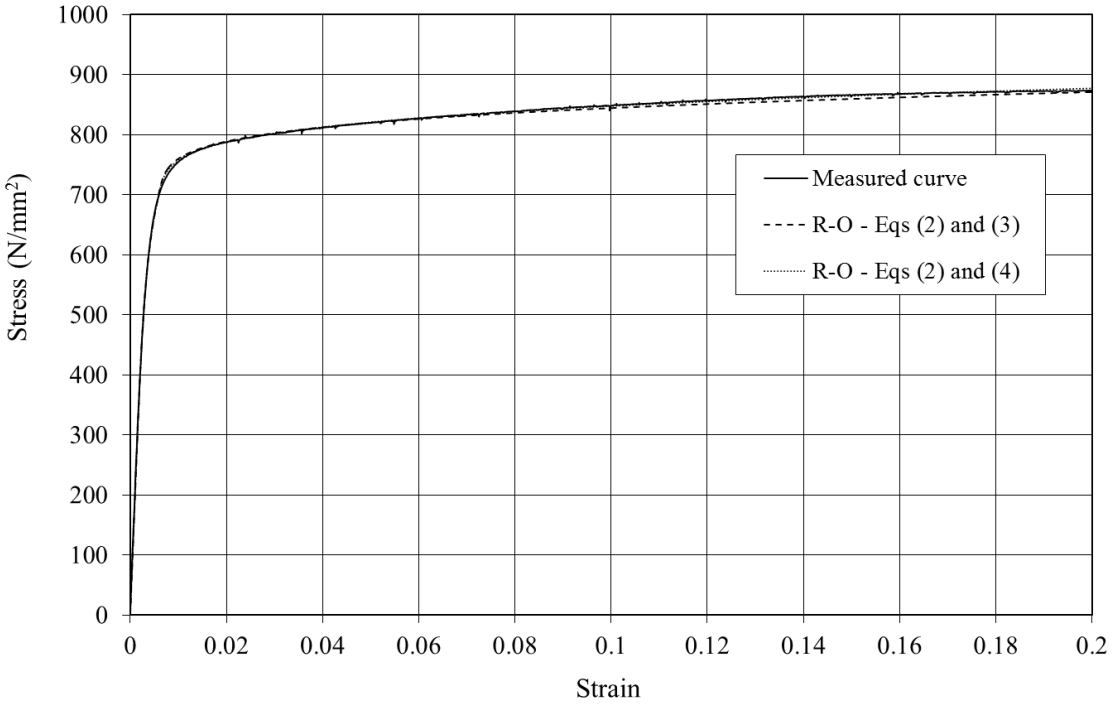

Figure 35 Comparison between a typical measured room temperature stress-strain curve and the two-stage Ramberg-Osgood models given by Eqs (2) and (3) [45,46,48] and Eqs (2) and (4) [49]

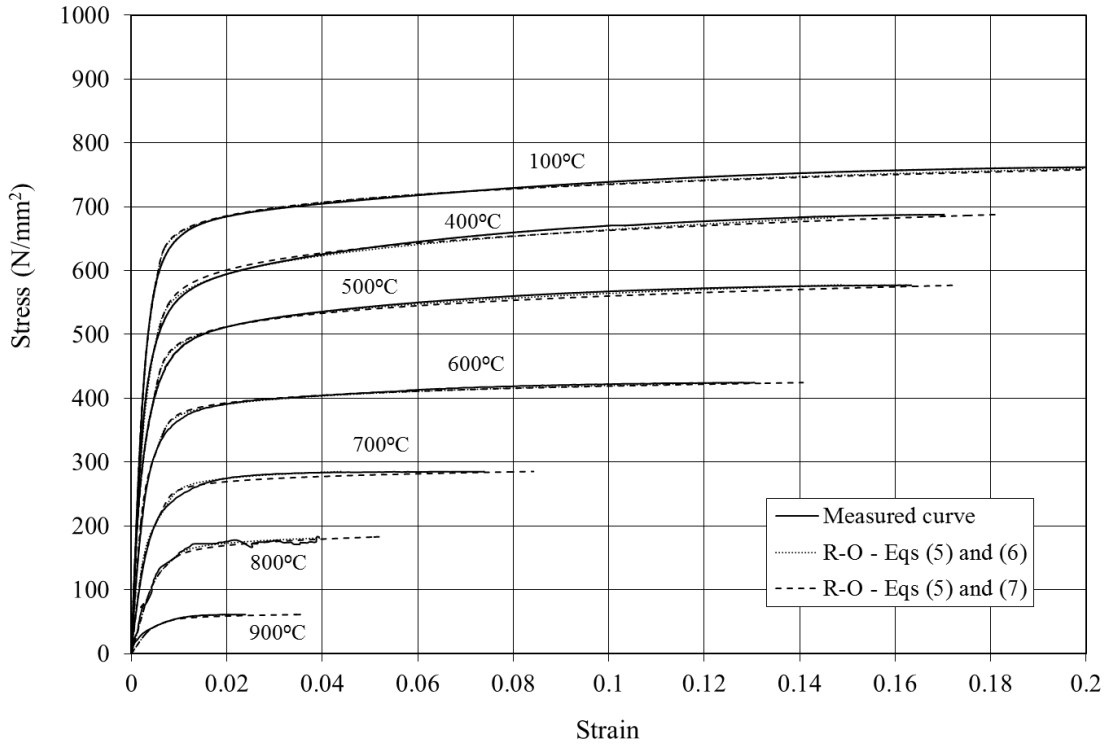

Figure 36 Comparison between typical measured elevated temperature stress-strain curves and the two-stage Ramberg-Osgood models given by Eqs (5) and (6) [39] and Eqs (5) and (7) [44]